Co-evolution of simian foamy viruses (SFVs) with primates: comparative functional analyses of miRNAs expressed from SFVs

(サルフォーミーウイルスと霊長類の共進化：サルフォーミーウイルス由来マイクロ RNA の比較機能解析)

後藤　暁

Biologicals 43 (2015) 363–368

Contents lists available at ScienceDirect

Biologicals

journal homepage: www.elsevier.com/locate/biologicals

Comparison between S+L− assay and LacZ marker rescue assay for detecting replication-competent gammaretroviruses

A. Hashimoto-Gotoh, R. Yoshikawa, T. Miyazawa*

Laboratory of Signal Transduction, Department of Cell Biology, Institute for Virus Research, Kyoto University, 53 Shogoin-Kawaharacho, Sakyo-ku, Kyoto 606-8507, Japan

ARTICLE INFO

Article history:
Received 23 December 2014
Received in revised form
29 April 2015
Accepted 15 June 2015
Available online 8 July 2015

Keywords:
S+L− assay
LacZ marker rescue assay
Endogenous retrovirus

ABSTRACT

To avoid contamination of adventitious gammaretroviruses in biological products such as vaccines, it is necessary to check the master seed cells for manufacturing. There are several assays to detect infectious gammaretroviruses. Among these, sarcoma-positive, leukemia-negative (S+L−) assay is a classical infectivity assay, which is often recommended in governmental guidelines. The S+L− cells used in S+L− assay generate unique focus upon the infection of replication-competent gammaretroviruses. Although S+L− assay is well recognized for the detection, their applicability is questionable in some cases. On the other hand, LacZ marker rescue (LMR) assay detects infectious gammaretroviruses by transducing LacZ marker gene to the target cells, which shows *lacZ*-positive foci if the infectious virus is present. In this study, we compared LMR and S+L− assays for detection of a variety of endogenous and exogenous gammaretroviruses. As results, LMR assay could detect all gammaretroviruses examined. On the other hand, S+L− assay using feline S+L− cells, termed QN10S, could not detect porcine endogenous retrovirus (PERV) subgroups A/B. Further, S+L− mink cells could not detect feline leukemia virus subgroups B in addition to PERV-A/B. These data indicate that LMR assay is better suited to detect wider range of gammaretroviruses.

1. Introduction

The contamination by infectious endogenous retroviruses (ERVs) is an emerging concern in biologicals, as the source of the viruses is the cell itself for manufacturing. In 2010, we showed the first evidence that an infectious endogenous gammaretrovirus, called RD-114 virus, is contaminated in live attenuated vaccines for companion animals, obtained either from Japan or the U.K. [1]. Although the potential of this contamination to provoke biohazard is less likely [1], such contamination needs to be prevented to reduce the risk of such incident. Therefore, it is important to develop appropriate detection methods to avoid ERV contamination.

Although the importance to prevent contamination by infectious ERVs is relatively recent recognition, there is a long history of incidents that biologicals are contaminated with exogenous gammaretroviruses. For instance, it was reported as early as 1976 that a Marek's disease vaccine was contaminated with reticuloendotheliosis virus (REV) [2]. It was further reported that those chickens received this contaminated vaccine developed symptoms that resemble reticuloendotheliosis rather than Marek's disease [3]. This indicates that such contamination by gammaretrovirus needs to be carefully examined to prevent the outbreak of unexpected retrovirus infection.

To avoid such contamination of adventitious gammaretroviruses, it is necessary to check the master seed cells for manufacturing. In order to carry out inspection, various techniques are employed to detect gammaretroviral contamination, such as reverse-transcriptase (RT) activity assay, RT-polymerase chain reaction (PCR) assay, transmission electron microscopy (TEM), and infectivity assay. For the gammaretroviruses already known, their presence can be easily detected by the use of RT-PCR and PCR. However, the PCR cannot detect the presence of unknown infectious gammaretroviruses. Although highly sensitive RT assays have been developed [4–6], the interpretation of the results is sometimes controversial due to the background level of the endogenous RT activity present in the cells. Also, the TEM has limitation, as the absence of viral particles observed in TEM does not warrant that the viral particles do not exist. Therefore, as well as these three techniques, the infectivity assay shares the important aspect of the viral

* Corresponding author. Tel./fax: +81 (0)75 751 4814.
E-mail address: takavet@gmail.com (T. Miyazawa).

http://dx.doi.org/10.1016/j.biologicals.2015.06.007
1045-1056/

detection. Infectivity assay detects the virus by applying the investigating samples to specific cell lines. Usually gammaretroviruses do not induce any visible cytopathic effects. To visualize the gammaretroviral infections, several assay systems have been developed. To date, sarcoma-positive leukemia-negative (S+L−) assay, one of such assays, is often recommended in governmental guidelines for quality control of manufactured biological products. For example, it is recommended in U.S. to monitor the presence of infectious gammaretroviruses in live attenuated viral vaccines as well as retrovirus/lentivirus vectors used for gene therapy [7,8].

The S+L− assay was first documented in 1971 by Bassin et al. describing that a group of murine 3T3 cells containing mouse sarcoma virus (MSV) genome induced foci when they were infected with replication-competent murine leukemia virus (MLV) [9]. This technique was first introduced as specialized assay to detect the presence of MLV, which does not induce transformation in susceptible cell lines. Later, it was shown that S+L− cell lines could be obtained not only in mice, but also in other species, such as QN10S cell line from cat [10] and S+L− mink cell line from mink [11]. Those S+L− cell lines contain "defective" MSV genome, which cannot replicate but can transform (r−t+) the host cells. Normally, this cell line shows flat cell morphology, because the MSV genome in the cells is marginally expressed below the level to transform the cells. However, once the MSV genome was "rescued" by the infection of r+t− viruses such as MLVs, it initiates transformation of cells to induce "foci" that can be easily detected under a microscope [12]. Thus, appearance of "focus" in S+L− cells after inoculation with a sample indicates the presence of infectious MLVs.

On the other hand, marker rescue assay is also recommended for screening of infectious MLVs in retrovirus/lentivirus vectors [8]. In marker rescue assay, the infectious gammaretrovirus can be identified by the presence of easily distinguishable marker transgenes, such as the *lacZ* gene for formation of blue-foci by x-gal staining. This idea was originally developed as a case study in gene therapy to show the evidence of gene transfer to the target tissues, by using *nls-lacZ* gene as a marker [13]. The *nls-LacZ* contains nuclear localization signal upstream from the open reading frame of the *LacZ* gene, and can be used as a "marker" to track the viral infection [14]. Fig. 1 summarizes the basis of LacZ marker rescue (LMR) assay. Firstly, to introduce *nls-LacZ* gene, pseudotype virus containing *nls-LacZ* gene as a viral genome is inoculated into investigating cells which had been persistently infected with infectious gammaretrovirus "X". In Fig. 1, TELCeB6/FBFeLV-B cells [15] is used as example to produce virus to transduce *nls-LacZ* gene into the cells, which harbors the envelope protein (Env) of feline leukemia virus subgroup B (FeLV-B) and viral core of Moloney MLV as well as *nls-LacZ* gene with a packaging signal from MLV. Then the *nls-LacZ* gene will be packaged into "X" viral particles, which leads to the generation of pseudotype virus *lacZ*(X). The *lacZ*(X) harbors the same viral proteins as in "X", but *nls-LacZ* gene is packaged which will show the blue foci formed by expressed β-galactosidase in nuclei upon β-gal staining. The LMR assay was already shown to be applicable to detection of infectious gammaretroviruses other than MLVs. For example, we applied the LMR assay for the detection of replication-competent RD-114 virus contaminated in live attenuated vaccines, as mentioned above [1,16].

Both assays have been well studied for the detection of infectious MLVs. For example, a study carried out in 1996 showed that both S+L− and LMR assays could detect MLV with equal virus titers [17]. However, the comparative study between these assays to validate the availability for the detection of other gammaretroviruses is still missing. As S+L− assay is recommended in many governmental guidelines, it is important to assess whether it is truly appropriate in the detection of infectious gammaretroviruses to avoid viral contamination, especially in many cell lines used to manufacture biological products. Moreover, availability of the genome databases and computer programs unveil novel ERVs in cell lines used in production of biological products, most of which are not characterized [18]. Among them, mouse cell lines, susceptible to MLVs or other infectious gammaretroviruses, had been used in a wide range of researches, such as feeder layer cells in culture of induced pluripotent stem (iPS) cells and embryonic stem (ES) cells. It is important to evaluate different assays for detection of infectious gammaretroviruses in such feeder layer cells to prevent the gammaretroviral infection in iPS and ES cells. In this study, we compared the virus titers as well as the availability of several different gammaretroviruses to be detected by S+L− and LMR assays, using 4 different cell lines: QN10S and S+L− mink cells for S+L− assay, and human embryonic kidney (HEK) 293T and TE671 cells for LMR assay. Further, we determined the minimal viral copy

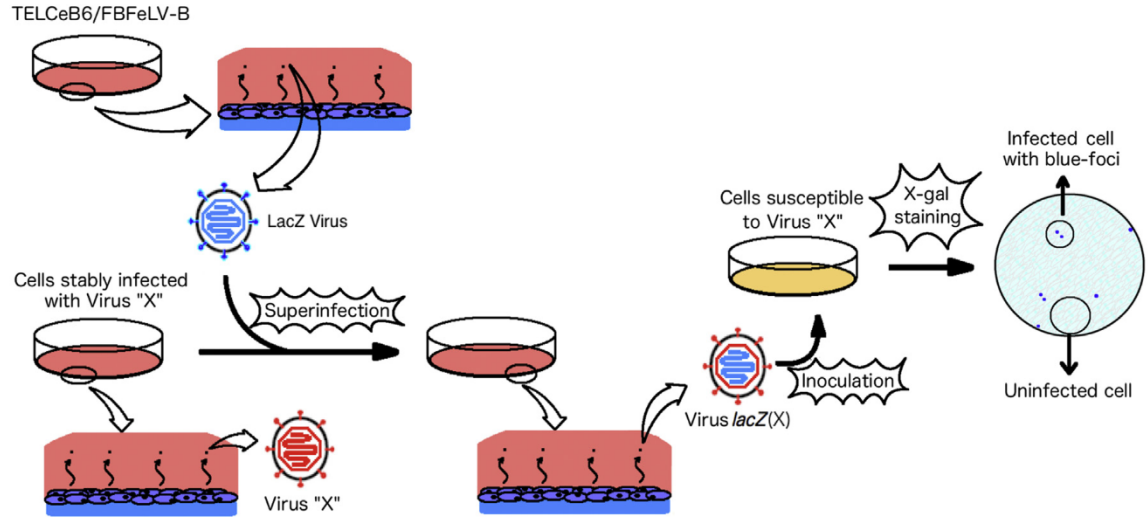

Fig. 1. Schematic illustration of LMR assay to detect infectious gammaretrovirus (here refer to as X virus) as example. (Left) *nls-LacZ* gene was introduced into cells stably infected with X virus by inoculating a helper-free LacZ pseudotype virus prepared from the culture supernatant of TeLCeB6/FBFeLV-B cells. (Middle) From the *nls-LacZ*-transduced cells, the pseudotyping of X virus termed *lacZ*(X) is produced. (Right) This pseudotype virus contains the Gag, Pol, Env proteins derived from original X virus, but only *nls-lacZ* gene as viral gene. Infection of *lacZ*(X) to naive cell lines susceptible to the virus causes the formation of the blue-foci in nuclei of infected cells.

numbers which could be detected by S+L− and LMR assays. Our study indicated that LMR assays could detect wider range of gammaretroviruses than S+L− assays with equal or higher virus titers.

2. Materials and methods

2.1. Cells

Human embryonic kidney (HEK) 293T (ATCC, CRL-11268) [19], HEK293 (ATCC, CRL-1573), TE671 (human rhabdomyosarcoma) [20], S+L− mink (RIKEN BRC: RBC 1834) [12], and QN10S (feline fibroblast cell line) cells [21,10], and a Platinum-E retroviral packaging cell line, termed Plat-E cells [22], were cultured in Dulbecco's modified Eagle's medium (DMEM) (Sigma–Aldrich, St. Louis, MO, U.S.A.) supplemented with 10% heat-inactivated fetal calf serum, penicillin (100 units/ml) and streptomycin (100 μg/ml) at 37 °C in 5% CO_2 in air using CO_2 incubators.

2.2. Viruses

Xenotropic MLV (X-MLV), RD-114 virus, FeLV subgroup A (FeLV-A), FeLV-B, FeLV-C, porcine endogenous retrovirus subgroup A (PERV-A), and PERV-B were obtained from TE671, HEK293T, or HEK293 cells persistently infected with X-MLV, RD-114 virus (TE671/X-MLV, RD-114), FeLV-A, FeLV-B, FeLV-C (HEK293T/FeLV-A, FeLV-B, FeLV-C), and PERV-A, PERV-B (HEK293/PERV-A, PERV-B), respectively. These cell lines were used to produce the *lacZ* pseudotyped viruses, which are: *lacZ*(X-MLV), *lacZ*(RD-114), *lacZ*(FeLV-A), *lacZ*(FeLV-B), *lacZ*(FeLV-C), *lacZ*(PERV-A) and *lacZ*(PERV-B). For all but *lacZ*(FeLV-B), the pseudotype viruses were produced by superinfection of infected cells with the culture supernatant of TELCeB6/FBFeLV-B cells which produce 'replication-incompetent' (helper-free) FeLV-B Env-pseudotyped virus containing *nls-LacZ* gene [15]. The *lacZ* pseudotype virus of FeLV-B, *lacZ*(FeLV-B), was obtained by superinfection of infected cell with the supernatant of Plat-E cells [22] transduced with *nls-LacZ* gene [Plat-E(LacZ) cells] transfected with an expression plasmid of vesicular stomatitis virus G protein using Lipofectamine 2000 (Life Technologies, MA, U.S.A.). All pseudotype viruses were collected after filtration with 450 nm membrane filters (PALL, MI, U.S.A.). The baboon endogenous retrovirus (BaEV) and its *lacZ* pseudotyped virus, *lacZ*(BaEV), were collected by transfecting HEK293T and HEK293T cells transduced with *nls-LacZ* gene [HEK293T(LacZ) cells] with an infectious molecular clone of M7 strain of BaEV [23] using Lipofectamine 2000 (Life Technologies). The transfected cells were passaged several times to ensure the cells had been stably infected.

2.3. LMR assay

The LMR assay was performed using TE671 or HEK293T cells as target cells as described previously [16]. Briefly, 1.6×10^5 of TE671 cells were plated on each well of regular 24-well plate (Thermo Scientific, MA, U.S.A.), and HEK293T cells were plated on each well of collagen-coated 24-well plate (Iwaki, Shizuoka, Japan) one day before inoculation. On the next day, each culture supernatant containing *lacZ* pseudotype virus was serially diluted and immediately inoculated into these cells under the presence of polybrene® (8 μg/ml), and the inoculated cells were incubated for viral adsorption for 4 h at 37 °C with 5% CO_2 in air. After inoculation, the inocula were replaced with 0.5 ml of fresh medium, and further incubated for additional two days. Cells were then fixed with 1% glutaraldehyde and stained with 1 mg/ml β-gal, and *lacZ*-positive foci were counted to titrate the pseudotype viruses as described previously [16]. This assay was performed in triplicate independently, and the statistical significance was assessed by student's *t*-test.

2.4. S+L− assay

The S+L− assay was conducted using QN10S or S+L− mink cells as described previously [12,21]. Briefly, 1×10^4 of QN10S/S+L− mink cells were plated on each well of regular 24-well plate (Thermo Scientific, MA, U.S.A.) one day before inoculation. Then each culture supernatant containing replication-competent virus was serially diluted and immediately inoculated into naïve cells under the presence of polybrene® (8 μg/ml), and incubated for 4 h at 37 °C with 5% CO_2 in air for viral adsorption. Then the inoculum was replaced with 1 ml of fresh medium, and further incubated for one week. Cells were then examined under a microscope to observe the appearance of foci, and positive foci were counted to titrate pseudotype viruses as described previously [21]. This assay was performed in triplicate, independently. The statistical significance was assessed by student's *t*-test.

2.5. Real-time reverse transcription (RT)-PCR

Real-time RT-PCR was carried out to determine the viral RNA copy numbers. The culture supernatant of *lacZ*(X-MLV)-producing cells was prepared as described in Section 2.2. The supernatant was treated with recombinant DNase I (Takara, Shiga, Japan) under the presence of RNase inhibitor (Takara, Shiga, Japan) to remove free DNA. This reaction was conducted in 37 °C for 60 min and then 75 °C for 10 min. Then, the RNA copy numbers of *lacZ*(X-MLV) were measured with ABI7500 (Applied Biosystems, Massachusetts, U.S.A.) using One Step SYBR® PrimeScript™ PLUS RT-PCR Kit (Takara, Shiga, Japan) according to the manufacturer's instruction. The primer was designed to amplify the *nls-LacZ* gene (5′-GCGTGGATGAAGACCAGC-3′ and 5′-CGAAGCCGCCCTGTAAAC-3′). The statistical significance was assessed by student's *t*-test.

3. Results

3.1. Morphology of foci in each assay

The morphology of foci formed in each assay is shown in Fig. 2. In S+L− assay, QN10S and S+L− mink cells showed distinctive morphologies of foci. In LMR assay, the blue stained cell-foci appear as a cluster of small blue dots (in the web version) which represent the expression of *nls-lacZ* gene of cells upon the β-gal staining (Fig. 2A). This indicates that the *lacZ* pseudotype virus infected the target cells, and *nls-lacZ* gene is successfully expressed. In QN10S cells, the focus appeared as a crater-like form, indicating that a group of cells are possibly peeled off from the plate in round-shaped fashion (Fig. 2B). On the other hand, the focus in S+L− mink cells showed the accumulation of cells at a particular site of plate, forming a random-shaped aggregate of cells (Fig. 2C).

3.2. Difference of virus detection in each assay

Difference was observed between the two assays in terms of virus detection. In LMR assay, all viruses tested showed the sign of *lacZ*-positive foci (Fig. 3). However, in S+L− assay, both QN10S and S+L− mink cells did not show any signs of transformation upon the infection by PERV-A and -B (Fig. 4). Moreover, FeLV-B did not show any foci at all in S+L− mink cells (Fig. 4). Comparison between S+L− assay and LMR assay showed that LMR assay detects all ERVs and X-MLV with higher viral titers than S+L− assay (Fig. 5).

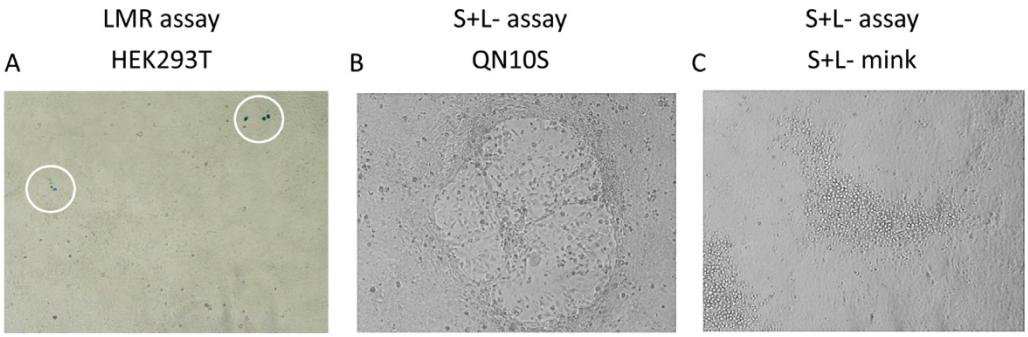

Fig. 2. Distinctive foci appeared in different infectivity assays. (A) Typical *lacZ* positive-foci formed in HEK293T cells by LMR assay. (B) Typical focus formed in QN10S cells by S+L− assay. (C) Typical focus formed in S+L− mink cells by S+L− assay.

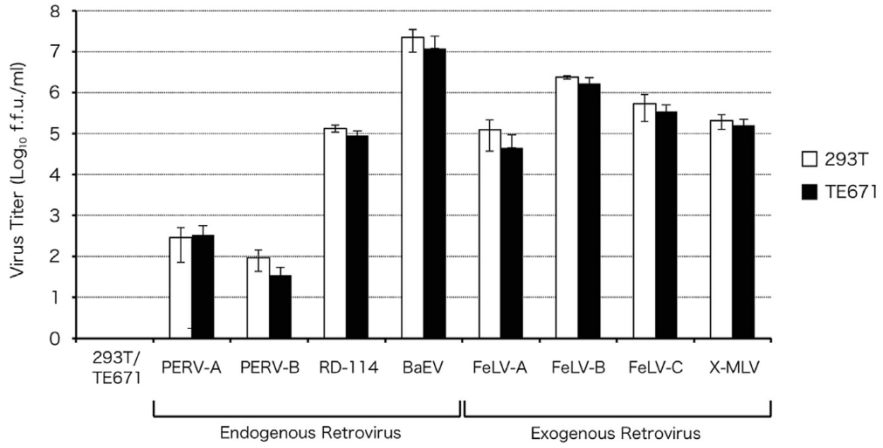

Fig. 3. LMR assay. LMR assay could titrate all viruses tested, with slightly higher virus titers in HEK293T cell. Each pseudotype virus was inoculated into either HEK293T (white bars) or TE671 cells (black bars). Viral titers were expressed as focus-forming units per milliliter (f.f.u./ml). The experiments were repeated independently for three times, and each set of data was used for calculation of mean standard deviation expressed as error bars. No significant difference was observed between 2 different cell lines used for the assay.

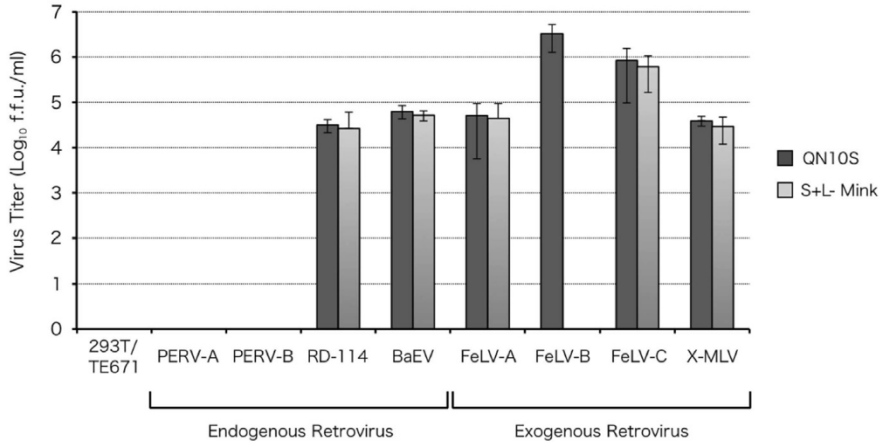

Fig. 4. S+L− assay. S+L− assay could not titrate PERV-A and B in both QN10S and S+L- mink cells. Moreover, FeLV-B was not detected in S+L− mink cells. Each virus was inoculated into either QN10S (thick gray bars) or S+L− mink cells (light gray bars). Viral titers were expressed as f.f.u./ml. The experiments were repeated independently for three times, and each set of data was used for calculation of mean standard deviation expressed as error bars. Apart from FeLV-B, no significant difference was observed between 2 different cell lines used for the assay.

3.3. *Real-time RT-PCR*

The real-time RT-PCR revealed that the RNA copy numbers of *lacZ*(X-MLV) was more than 10^8/ml (Fig. 6). As negative control, the culture supernatant of TE671 cells transduced with *nls-LacZ* gene was used.

4. Discussion

Our results showed that LMR assay can detect a wider range of infectious gammaretroviruses than S+L− assay, at least among the viruses we examined in this study. For the viruses which both assays could detect, both assays showed comparable virus titers, or

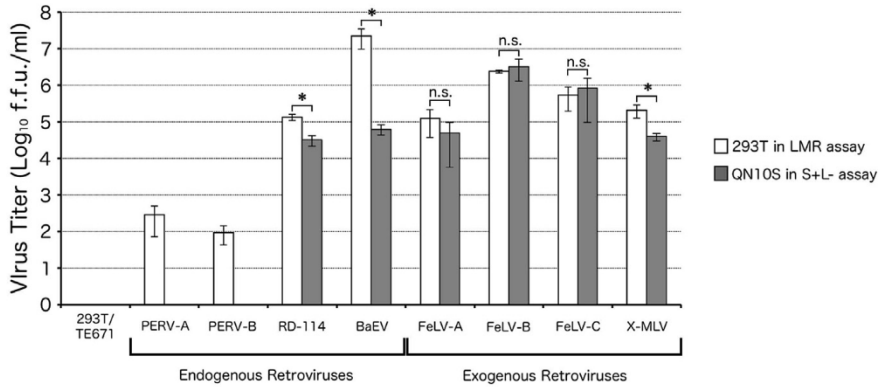

Fig. 5. Comparison of virus titers determined by LMR and S+L− assays. LMR assay using HEK293T cells and S+L− assay using QN10S cells were compared. The asterisks indicate that *p* value calculated by student *t*-test was less than 0.05, and "n.s." indicates there were statistically no significant differences between these values.

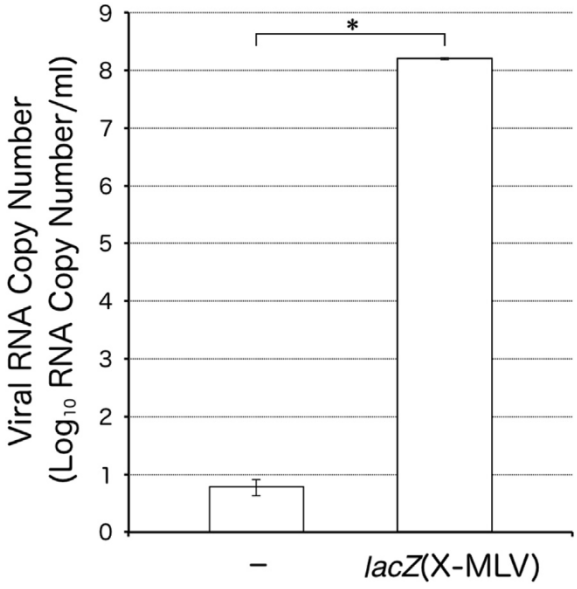

Fig. 6. Real-time RT-PCR of *lacZ*(X-MLV). The viral RNA copy number of *lacZ*(X-MLV) was measured by real-time RT-PCR. The culture supernatant of TE671 cells transduced with *nls-LacZ* gene was used as negative control (−). The asterisk indicates that *p* value calculated by student *t*-test was less than 0.0001.

sometimes higher in LMR assay than S+L− assay, correlating with a previous study conducted for the detection of MLVs [17]. Except that S+L− assay with QN10S cells showed slightly higher virus titers in FeLV-B and C than LMR assay, the LMR assay with HEK293T cell showed the highest virus titers overall, including PERV-A/B which were only detectable in LMR assay. The RT-PCR result showed that there are approximately 10^8 viral RNA copies/ml in the *lacZ*(X-MLV) solution (Fig. 6). On the other hand, approximately 10^5 f.f.u./ml of infectivity was observed from the same virus solution when either LMR or S+L− assay was used. This indicates that there must be approximately 10^3 viral RNA copies to detect one focus-forming virus in each assay.

Although RT-PCR requires thousand-fold less viral RNA copy numbers for detection, it should be noted that RT-PCR detects both infectious and uninfectious virus particles. In other words, RT-PCR does not specifically distinguish infectious virus from uninfectious virus. Because RT-PCR detects uninfectious ERV particles which most cells produce, infectious assays should be regarded as vital assay to monitor the infectious virus contamination in master seed cells.

PERV-A/B are porcine ERVs which received attention for its possible production in the transplanted pig organs in xeno-transplantation. Although there are no reports showing that PERVs had infected the recipients, the possible recombination of PERVs and other ERVs or exogenous retroviruses to gain infectivity remains as a risk of xenotransplantation from pigs [24]. The inability of S+L− assay to detect the presence of PERVs suggests that such possible production of PERVs in donors cannot be prevented if S+L− assay was used as the standard of infectivity assay to detect infectious PERVs.

The other issue with regards to the S+L− assay is that their limit of virus detection is significantly different between the S+L− cell lines used. For example, FeLV-B exhibited quite high titer when it was titrated in the QN10S cells, but completely no activity in S+L− mink cells. The strain of FeLV-B used in our study is derived from an infectious molecular clone of FeLV-B strain Gardner-Arnstein. This difference indicates that the particular type of S+L− cells recommended in governmental guidelines cannot detect certain infectious gammaretrovirus which is detectable in other cell lines. For example, Ministry of Health, Labor and Welfare of Japan not only recommends to use S+L− assay, but also specifically states to use S+L− mink cell line for the infectivity assay in mouse feeder cells used for tissue engineering in their guideline [25]. As this specifically recommends the use of S+L− mink cell line, possible FeLV-B contamination could not be detected. This property of S+L− assay will also need to be reevaluated for the quality control of biological products to avoid viral contamination.

Although our results showed that LMR assay could detect a wider range of infectious gammaretroviruses, it is important that the other types of retroviruses are also potent contaminants. For example, it is well recognized that avian leukosis virus (ALV), alpharetrovirus in birds, had been contaminated in the past for several vaccines for yellow fever, mumps, and measles [26,27]. In order to detect ALV contamination, LMR is not a good option because the current LMR assay system cannot detect alpharetroviruses. This is due to the difference in the packaging signals between alpharetroviruses and gammaretroviruses. Moreover, gammaretroviruses are not the only retroviruses which are supposed to be contaminated in biologicals. For example, mice mainly harbor betaretroviruses as their endogenized retrovirus populations [28]. This fact indicates that negative results by LMR assay in suspicious mouse cell lines cannot exclude the possibility of contamination by infectious betaretroviruses. Development of other methods for detection of betaretroviruses is vital to address the safety in this regard. On the other hand, some other viruses, such as REV, might be ideal target of LMR assay. It was previously

reported that a Marek's disease vaccine had been contaminated with REV and subsequently reticuloendotheliosis-like symptom had been observed in the recipients [3]. Since REV is a gammaretrovirus in birds [29], LMR assay should be useful to detect REV in biological materials.

In this study, LMR assay with HEK293T cells is the best for detection of infectious gammaretroviruses in terms of wide range of the viruses to be detected. The reason why so many viruses could be detected in this assay is that the basis of focus-formation in S+L− assay is different from that of LMR assay. In S+L− assay, the virus needs to infect as well as multiply in numbers, so that it can initiate the focus-formation. By contrast, LMR assay only requires the infection but not multiplication for the expression of *lacZ* in cells, which can be detected as blue foci upon β-gal staining. This suggests that LMR assay is better suited for the detection and titration of gammaretroviruses that will not multiply or multiply in low speed, whereas S+L− assay is not suited to detect such viruses. Overall, our results indicate that LMR assay should be used for the detection of infectious gammaretroviruses to prevent the viral contamination in biological products such as mouse feeder layer cells used in iPS cell generation.

Acknowledgments

We are grateful to Dr. Yasuhiro Takeuchi (University College London, London, U.K.) for providing TELCeB6 cells, TE671/X-MLV, TE671/RD-114, HEK293/PERV-A and HEK293/PERV-B. We also thank Prof. James C Neil for providing infectious molecular clones of FeLV-A, FeLV-B and FeLV-C.

References

[1] Miyazawa T, Yoshikawa R, Golder M, Okada M, Stewart H, Palmarini M, et al. Isolation of an infectious endogenous retrovirus in a proportion of live attenuated vaccines for pets. J Virol 2010;84:3690–4.
[2] Yuasa N, Yoshida I, Taniguchi T. Isolation of a reticuloendotheliosis virus from chickens inoculated with Marek's disease vaccine. Natl Inst Anim Health Q (Tokyo) 1976;16:141–51.
[3] Taniguchi T, Yuasa N, Sato S, Horiuchi T. Pathological changes in chickens inoculated with reticuloendotheliosis-virus-contaminated Marek's disease vaccine. Natl Inst Anim Health Q (Tokyo) 1977;17:141–50.
[4] Heneine W, Yamamoto S, Switzer WM, Spira TJ, Folks TM. Detection of reverse transcriptase by a highly sensitive assay in sera from persons infected with human immunodeficiency virus type 1. J Infect Dis 1995;171:1210–6.
[5] Silver J, Maudru T, Fujita K, Repaske R. An RT-PCR assay for the enzyme activity of reverse transcriptase capable of detecting single virions. Nucleic Acids Res 1993;21:3593–4.
[6] Pyra H, Böni J, Schüpbach J. Ultrasensitive retrovirus detection by a reverse transcriptase assay based on product enhancement. Proc Natl Acad Sci U S A 1994;91:1544–8.
[7] Briefing document—testing for replication competent retrovirus (RCR)/lentivirus (RCL) in retroviral and lentiviral vector based gene therapy products—revisiting current FDA recommendations. US Food and Drug Administration; 2010. p. 1–18.
[8] Guidance for industry – characterization and qualification of cell substrates and other biological materials used in the production of viral vaccines for infectious disease indications. US Food and Drug Administration; 2010. p. 1–47.
[9] Bassin RH, Tuttle N, Fischinger PJ. Rapid cell culture assay technique for murine leukemia viruses. Nature 1971;229:564–6.
[10] Jarrett O, Ganière JP. Comparative studies of the efficacy of a recombinant feline leukaemia virus vaccine. Vet Rec 1996;138:7–11.
[11] Peeble PT, Gerwin BI, Parageorge AG, Smith SG. Murine sarcoma virus defectiveness: viral polymerase expression in murine and nonmurine host cells transformed by S+L− type murine sarcoma virus. Virology 1975;67:344–55.
[12] Peeble PT. An in vitro focus-induction assay for xenotropic murine leukemia virus, feline leukemia virus C, and the feline-primate viruses RD-114/CCC/M-7. Virology 1975;67:288–91.
[13] Ferry N, Duplessis O, Houssin D, Danos O, Heard JM. Retroviral-mediated gene transfer into hepatocytes *in vivo*. Proc Natl Acad Sci U S A 1991;88:8377–81.
[14] Cosset F-L, Takeuchi Y, Battini JL, Weiss RA, Collins MK. High-titer packaging cells producing recombinant retroviruses resistant to human serum. J Virol 1995;69:7430–6.
[15] Nakata R, Miyazawa T, Shin YS, Watanabe R, Mikami T, Matsuura Y. Reevaluation of host ranges of feline leukemia virus subgroups. Microbes Infect 2003;5:947–50.
[16] Sakaguchi S, Okada M, Shojima T, Baba K, Miyazawa T. Establishment of a LacZ marker rescue assay to detect infectious RD114 virus. J Vet Med Sci 2008;70:785–90.
[17] Forestell SP, Dando JS, Böhnlein E, Rigg RJ. Improved detection of replication-competent retrovirus. J Virol Methods 1996;60:171–8.
[18] Shepherd AJ, Wilson NJ, Smith KT. Characterisation of endogenous retroviruses in rodent cell line used for production of biologicals. Biologicals 2003;4:251–60.
[19] Graham FL, Smiley J, Russell WC, Nairn R. Characteristics of a human cell line transformed by DNA from human adenovirus type 5. J Gen Virol 1977;1:59–74.
[20] Stratton MR, Darling J, Pilkington GJ, Lantos PL, Reeves BR, Cooper CS. Characterization of the human cell line TE671. Carcinogenesis 1989;10:899–905.
[21] Sakaguchi S, Baba K, Ishikawa M, Yoshikawa R, Shojima T, Miyazawa T. Focus assay on RD114 virus in QN10S cells. J Vet Med Sci 2008;70:1383–6.
[22] Morita S, Kojima T, Kitamura T. Plat-E: an efficient and stable system for transient packaging of retroviruses. Gene Ther 2000;12:1063–6.
[23] Yoshikawa R, Miyaho R, Hashimoto A, Abe M, Yasuda J, Miyazawa T. Suppression of production of baboon endogenous virus by dominant negative mutants of cellular factors involved in multivesicular body sorting pathway. Virus Res 2015;196:128–34.
[24] Levy MF, Argaw T, Wilson CA, Brooks J, Sandstrom P, Merks H, et al. No evidence of PERV infection in healthcare workers exposed to transgenic porcine liver extracorporeal support. Xenotransplantation 2007;14:309–15.
[25] Guideline of the tissue engineering of epithelial tissue using either 3T3J2 or 3T3NIH cells for feeder cell, based on “guideline with regards to how the implementation of xenotransplantation can elicit problem of infectious disease in public health ”. Japan: Japan Ministry of Health, Labor, and Welfare; 2003. http://www.mhlw.go.jp/general/seido/kousei/i-kenkyu/isyoku2/sisin.html [in Japanese].
[26] Tsang SX, Switzer WM, Shanmugam V, Johnson JA, Goldsmith C, Wright A, et al. Evidence of avian leukosis virus subgroup E and endogenous avian virus in measles and mumps vaccines derived from chicken cells: investigation of transmission to vaccine recipients. J Virol 1999;73:5843–51.
[27] Hussain AI, Johnson JA, Da Silva Freire M, Heneine W. Identification and characterization of avian retroviruses in chicken embryo-derived yellow fever vaccines: investigation of transmission to vaccine recipients. J Virol 2003;77:1105–11.
[28] Hayward A, Cornwallis CK, Jern P. Pan-vertebrate comparative genomics unmasks retrovirus macroevolution. Proc Natl Acad Sci U S A 2015;112:464–9.
[29] Niewiadomska AM, Gifford RJ. The extraordinary evolutionary history of the reticuloendotheliosis viruses. PLoS Biol 2013;11:e1001642.

Persistent Infection of Simian Foamy Virus Derived from Japanese Macaque Leads to the High-Level Expression of microRNA that Resembles miR-1 microRNA Precursor Family

AKIRA HASHIMOTO-GOTOH[1], KOICHI KITAO[1], and TAKAYUKI MIYAZAWA[1,2*]

[1]*Laboratory of Virus-Host Coevolution, Institute for Frontier Life and Medical Sciences, Kyoto University, Kyoto 606-8507, Japan*

[2]*International Research Unit of Advanced Future Studies, Kyoto University, Kyoto 606-8502, Japan*

Topic: Microbial interactions and interrelations with other organisms (symbiosis)

Running heading: miRNAs of Japanese macaque's foamy virus

Correspondence to: Takayuki Miyazawa, Laboratory of Virus-Host Coevolution, Institute for Frontier Life and Medical Sciences, Kyoto University, 53 Shogoin-Kawaharacho, Sakyo-ku, Kyoto 606-8507, Japan.

E-mail: takavet@infront.kyoto-u.ac.jp

TEL/FAX: +81-(0)75-751-4814

Abstract

MicroRNAs (miRNAs) are a group of small non-coding RNAs and suppress the expression of target mRNAs. The seed sequence of miRNA plays a crucial role in recognizing the 3′-untranslated region of the target mRNA. It was previously reported that cells infected with a simian foamy virus (SFV) isolated from an African green monkey (*Chlorocebus aethiops*) (SFVcae) showed high expression of viral miRNAs encoded in the long terminal repeat of SFVcae. In this study, we investigated the roles and expression of miRNAs derived from an SFV isolated from a Japanese macaque (*Macaca fuscata*) (SFVmfu) using next-generation sequencing technologies. As results, SFVmfu also expressed viral miRNAs; however, the seed sequences of most miRNAs derived from SFVmfu were different from those from SFVcae reported previously. The cells persistently infected with SFVmfu highly expressed an miRNA that has the same seed sequence with the miR-1 microRNA precursor family. Luciferase reporter assays indicated that this miRNA downregulates the expression of the adenylyl cyclase-associate protein 1, which is upregulated in several solid tumors. Our study suggests that SFVmfu might utilize viral miRNAs to establish long-term coexistence with Japanese macaque.

Keywords: simian foamy virus, microRNA, miR-1 microRNA precursor family, adenylyl cyclase associated protein 1

Simian foamy virus (SFV) is a non-pathogenetic retrovirus that belongs to the genus *Simiispumavirus*, sub-family *Spumaviridae,* family *Retroviridae* (Khan *et al.,* 2018). The infection of SFV is commonly observed across the primates (Pinto-Santoni *et al.,* 2017). Compared to the other retroviruses belonging to sub-family *Orthoretroviridae*, the mutation rate of foamy viruses (FVs) is extremely low (1.7×10^{-8} substitution/site/year) and the phylogenetic tree of SFVs from various host species is congruent with that of the hosts, which indicates that SFV undergoes co-speciation with the host primate species (Switzer *et al.,* 2005; Liu *et al.,* 2008). The fact that SFVs and host primates have co-existed for millions of years indicates that there might be a symbiotic relationship between them.

MicroRNAs (miRNAs) are a group of small non-coding RNAs that are transcribed by RNA polymerase II or III (Abdelfattah *et al.,* 2014). The processed mature miRNAs will be incorporated into a series of proteins, such as the Argonaute, to form the RNA-induced silencing complex (RISC) (Chendrimada *et al.,* 2005). Once incorporated into RISC, one of the miRNA strands (3 prime (p) or 5p) will serve as a “guide” to recognize the complementary sequence present in the 3′-untranslated region (3′UTR) of target mRNA, and the expression of target gene will be repressed by RISC via deadenylation-mediated decay (Eulalio *et al.,* 2009). Notably, the seed sequences of miRNAs (nucleotides at 2-7 or 8 bases from the 5′-terminal) are perceived as the critical component for miRNA-induced RISC-targeting (Bartel, 2009).

Long terminal repeats (LTRs) are repetitive sequences present in both ends of the proviral DNA of retroviruses. LTR is composed of three regions; U3, R, and U5 (Fig. 1B): the U3 region contains the enhancer and promoter elements; the R region starts from the transcription start site (TSS) and contains the polyadenylation signal (Thompson *et al.,* 2016). The lengths of LTRs (particularly the U3 region) of FVs are longer than those of the other retroviruses. The U3 region of FVs partially overlaps with an ORF (termed ORF-2) encoding an auxiliary gene of FVs (Fig. 1B). Recently, it was reported that SFV LTR encodes miRNAs, which are expressed upon infection (Kincaid *et al.,* 2014). Not only SFV but also several retroviruses express miRNAs upon infection. These viruses include bovine leukemia virus, avian leukosis virus, human immunodeficiency virus 1, and bovine FV (Klase *et al.,* 2007; Kincaid *et al.,* 2012; Whisnant *et al.,* 2014; Yao *et al.,* 2014). Notably, miRNAs encoded in the LTRs of SFV and bovine FV include unique dumbbell-shaped pre-miRNAs that are derived from the transcripts that contain two adjacent pre-miRNAs separated by just a few bases (Kincaid *et al*., 2014; Whisnant *et al*., 2014). The dumbbell-shaped miRNAs derived from the LTR U3 region of FVs are shown to repress the expression of target genes (Cao *et al.,* 2018). Therefore, the miRNAs of FVs are supposed to play roles in viral replication and persistent infection; however, the functions of the miRNAs are still unclear at present.

74 The miRNAs derived from the LTR of SFV isolated from an African green monkey
75 (*Chlorocebus aethiops*) (SFVcae) has been extensively analyzed (Kincaid *et al.*, 2014).
76 However, the LTR is less conserved than the other viral genes in SFVs (Galvin *et al.*,
77 2013). Distinct SFVs might express miRNAs with different seed sequences that target
78 different genes. Here, we report the analyses of the miRNAs of SFV derived from a
79 Japanese macaque (*Macaca fuscata*) (SFVmfu). This virus was previously abbreviated as
80 SFVjm (Yoshikawa *et al.,* 2014), which was later renamed as SFVmfu (Khan *et al.,* 2018).
81 We revealed that the miRNAs are also expressed from the LTR of SFVmfu. Nevertheless,
82 the seed sequences of the miRNAs derived from SFVmfu were different from those of
83 SFVcae. Notably, an miRNA that was expressed at the highest level in SFVmfu shared the
84 seed sequence with the miR-1 miRNA precursor family of the host. Transcriptome and
85 immunoblot analyses and reporter assays indicated that the adenylyl cyclase-associated
86 protein 1 (CAP1) is one of the targets of the miRNA.

Materials and Methods

Cells and viruses

Human embryonic kidney (HEK) 293T (ATCC, CRL-11268) (Graham *et al*., 1977), TE671 (derived from human rhabdomyosarcoma) (ATCC, HTB-139) (Stratton *et al.,* 1989), and *M. dunni* (Clone III8C) cells (derived from skin fibroblasts of *Mus terricolor*) (ATCC, CRL-2017) (Lander and Chattopadhyay, 1984) were cultured in Dulbecco's modified Eagle's medium (Sigma Aldrich, St. Louis, MO, U.S.A.) supplemented with 10% heat-inactivated fetal calf serum, penicillin (100 units mL^{-1}) and streptomycin (100 mg mL^{-1}) (Invitrogen, Carlsbad, CA, U.S.A.) at 37°C in a humidified atmosphere of 5% CO_2 in air. An SFVmfu indicator cell line (*M. dunni* cells encoding β-galactosidase gene driven by the SFVmfu LTR), termed MD(SFVmfu-*lacZ*) cells, was newly established using the same approach as previously described (Lambert *et al*., 2016). The MD(SFVmfu-*lacZ*) cells were cultured in the same medium as above, except that puromycin (5 μg mL^{-1}) was added. To prepare stock viruses of SFVmfu strain WK1, *Mus dunni* cells were transfected with an infectious molecular clone (named pJM356) (Yoshikawa *et al*., 2014) of the strain using Lipofectamine 2000 (Thermo Fisher Scientific, Waltham, MA, U.S.A.) according to the manufacturer's instruction. The transfected cells were further cultured until syncytial foci became prominent. Then the cells were freeze-thawed three times and sonicated to release intracellular virus particles. The cell debris was removed by centrifugation at 3,000

106 rpm for 10 min, and the viruses were collected as stock viruses by filtrating with 450 nm
107 membrane filters (GVS, Mellishaw, LA, U.K.). The stock viruses were stored at -80°C until
108 use.
109
110 *Titration of SFVmfu*
111 To titrate stock viruses of SFVmfu, the LacZ assay was performed using the
112 MD(SFVmfu-*lacZ*) cells as the indicator cells. Briefly, 2×10^4 of MD(SFVmfu-*lacZ*) cells
113 were plated in each well of a 96-well plate (Thermo Fisher Scientific) one day before the
114 inoculation. On the next day, the stock viruses were serially diluted and immediately
115 inoculated into these cells under the presence of polybrene (8 μg mL^{-1}), and the inoculated
116 cells were incubated for viral absorption for four h at 37°C in a humidified atmosphere of
117 5% CO_2 in air. After inoculation, the inocula were replaced with 0.2 mL of fresh medium,
118 and further incubated for an additional two days. Cells were then fixed with 1%
119 glutaraldehyde and stained with X-Gal (5-bromo-4-chloro-3-indolyl-β-D-
120 galactopyranoside), and *lacZ*-positive foci were counted for titration as described
121 previously (Sakaguchi *et al.,* 2008; Hashimoto-Gotoh *et al.,* 2015).
122
123 *Establishment of TE671 cells persistently infected with SFVmfu*

TE671 cell persistently infected with SFVmfu strain WK1 (clone JM356) was established as described previously (Miyazawa *et al.,* 1995). Briefly, SFVmfu was inoculated into TE671 cells at a multiplicity of infection (MOI) of 0.172. The cells were cultured and passaged several times until severe cytopathic effects (syncytial formation and cell death) were observed. After most of the cells were detached from the culture plate, surviving cells were co-cultured with uninfected TE671 cells. The co-cultured cells continued to grow, showing mild cytopathic effects. After several passages, the cells were able to be passaged regularly (2-4-fold dilution per 4-5 days). Then we designated the cells as TE671/SFVmfu(PI) cells.

Construction of plasmids

Genomic DNAs were extracted from uninfected TE671 and TE671/SFVmfu(PI) cells using the QIAamp DNA Blood Mini kit (QIAGEN, Hilden, Germany). The genomic DNAs were used as the templates to construct miRNA expression plasmids. All primers used in this study are listed in Table S1. PCRs were carried out using KOD-Plus-Neo (Toyobo, Osaka, Japan) according to the manufacturer's instruction. For PCR, we used 200 μL thin-walled tubes and a C1000 thermal cycler (Bio-Rad Laboratories, Hercules, CA, U.S.A.). For hsa-mir-1, the amplified fragment was cloned into pcDNA3.1(+) digested with *Xba*I/*Xho*I to become pcDNA3.1(+)/hsa-mir-1 (Fig. 3A [top]). For SFVmfu-mir-S6-7, the

amplified fragment was cloned into pUC18 digested with *Hin*dIII/*Bam*HI to become pUC18/SFVmfu-mir-S6-7 (Fig. 3A [center]).

A series of firefly luciferase reporter plasmids was constructed with inserts at the 3′-end of firefly luciferase. Briefly, the human cytomegalovirus (hCMV) enhancer/promoter was cloned into the *Nhe*I/*Hin*dIII sites of pGL3-basic (Promega, Madison, WI, U.S.A.) to become pGL3-hCMV (Fig. 3A [bottom]). The complementary sequence of each mature miRNA (hsa-miR-1 or SFVmfu-miR-S7-5p) was prepared by annealing and extending the synthetic oligo and cloned into the *Xba*I site of the pGL3-hCMV using NEBuilder HiFi DNA Assembly (New England Biolab, Ipswich, MA, U.S.A.) to become pGL3-hCMV/hsa-miR-1 or pGL3/hCMV/SFVmfu-miR-S7-5p (Fig. 3A [bottom]). Similarly, the 3′UTR of human CAP1 was cloned into the *Xba*I site of the pGL3-hCMV to become pGL3-hCMV/CAP1 3′UTR (Wild-type) (Fig. 4A). Using the pGL3-hCMV/CAP1 3′UTR (Wild-type) as a template, site-directed mutagenesis was carried out at the hsa-miR-1/SFVmfu-miR-S7-5p recognition sites within the CAP1 3′UTR to become pGL3-hCMV/CAP1 3′UTR (Single mutant [mut.]) and pGL3-hCMV/CAP1 3′UTR (Triple mut.) (Fig. 4A). The recognition sites were predicted using an online database miRDB version 6.0 (http://www.mirdb.org/) (Wong and Wang, 2015; Liu and Wang, 2019).

Next-generation sequencing analyses

Small RNA sequencing and transcriptome analyses were performed in TE671 and TE671/SFVmfu(PI) cells. Total RNAs were extracted from the cells using RNAzol (Promega), followed by DNase I (Roche, Basel, Switzerland) treatment without a heat inactivation step, and re-extracted using RNAzol. The re-extracted RNAs were further processed by a commercial next-generation sequencing company (Novogene, Beijing, China).

For small RNA sequencing, the sequencing libraries were constructed from the total RNAs using the NEBNext Multiplex Small RNA Library Prep Set for Illumina (New England Biolab) which generates strand-specific small RNA libraries. Size selection of the cDNA libraries was performed by native polyacrylamide gel (12%)-electrophoresis to isolate a fraction containing miRNA-derived cDNAs. Then, the single-end 50 bp sequencing was performed on an Illumina Hiseq 2500 platform. The sequencing adapter sequences were trimmed from the pre-processed reads using Trimmomatic (ver. 0.38) followed by Fastp (ver. 0.19.4) (Bolger *et al.,* 2014; Chen *et al.,* 2018). Then, the reads were mapped to the viral genome of SFVmfu clone JM356 (Yoshikawa *et al.*, 2014) using Bowtie2 (ver. 2.3.4.3) (Langmead and Salzberg, 2012) and converted to the bam file using Samtools (ver. 1.9) (Li *et al.,* 2009). The bam files were converted to bed files, and the coverage depth was calculated using Bedtools (ver. 2.28.0) (Quinlan and Hall, 2010). The secondary structures of miRNA were predicted using RNAfold with default parameters (Gruber *et al.,* 2008;

181 Lorenz *et al.,* 2011). The coverage depth was visualized using Microsoft Excel (ver.
182 16.28).
183 For transcriptome analyses, the sequencing libraries were constructed using the
184 NEBNext Ultra RNA Library Prep Kit for Illumina (New England Biolab) which generates
185 non-strand-specific cDNA libraries. Then, the paired-end 150 bp sequencing was
186 performed on an Illumina Hiseq 2500 platform. The reads were mapped to the human
187 genome (GRCh38.p12) using Hisat2 (ver. 2.1.0) (Kim *et al.,* 2015) and converted to bam
188 file using Samtools (ver. 1.9) (Li *et al.,* 2009). The mapped reads were assembled using
189 Cufflinks (ver. 2.1.1), and expression differences between uninfected TE671 and
190 TE671/SFVmfu(PI) cells were calculated using Cuffmerge (ver. 2.1.1) and Cuffdiff (ver.
191 2.1.1) (Trapnell *et al.,* 2010; Trapnell *et al.,* 2012). The potential targets of SFVmfu-miR-
192 S7-5p were predicted using an online database miRDB version 6 (Wong and Wang, 2015;
193 Liu and Wang, 2019). The calculated expression levels were visualized using Microsoft
194 Excel (ver. 16.28).
195
196 *Multiple sequencing alignment analyses of CAP1 3′UTRs and SFV LTRs from various*
197 *species*
198 Genomic DNA of a Japanese macaque was extracted from blood using the QIAamp
199 DNA Blood Mini kit (QIAGEN). Extracted DNA was used as a template to amplify 3′UTR of

200 CAP1 by PCR using primers listed in Table S1. The amplified product was cloned into
201 *Hin*dIII/*Eco*RI sites of pcDNA3.1(+). The reverse primer used for the PCR was applied for
202 sequencing. Sequencing analysis was performed by a commercial DNA sequencing
203 company (Fasmac, Kanagawa, Japan). The 3′UTR sequences of CAP1 from human
204 (*Homo sapiens*), African green monkey (AGM), crab-eating macaque (*Macaca*
205 *fascicularis*), rhesus macaque (*Macaca mulatta*) were retrieved from ENSEMBL release 97
206 (human: GRCh38.p12, vervet AGM: ChlSab1.1, crab-eating macaque:
207 Macaca_fascicularis_5.0, rhesus macaque: Mmul_8.0.1) (Accessed in July 2019).
208 The LTR sequences of the following SFVs were retrieved from the National Center of
209 Biotechnology Information: SFVcae_LK3 (NC_010820), SFVmcy_FV34 (KF026286.1),
210 SFVmmu_DPZ9524 (MG051205.1) and SFVmfu_WK1.pJM356 (NC_039026.1), which are
211 derived from AGM, Taiwanese macaque (*Macaca cyclopis*), rhesus macaque, and
212 Japanese macaque, respectively.
213 The multiple sequence alignment analyses of CAP1 3′UTRs and SFV LTRs were
214 carried out using the MAFFT program (ver. 7.407) with the L-INS-i method (Katoh and
215 Standley, 2013). The aligned sequences were visualized using Seaview (ver. 4.7) (Gouy *et*
216 *al.,* 2010).
217
218 *Immunoblot analyses*

219 At 48 h or 96 h after either mock- or SFVmfu-infection (at an MOI of 0.34), the whole-
220 cell lysates of TE671 cells were obtained with RIPA buffer (50 mM Tris-Cl [pH 7.4], 150
221 mM NaCl, 5 mM EDTA, 1% Nonidet P-40, 1% sodium deoxycholate, 0.1% sodium dodecyl
222 sulfate, 1% aprotinin, 50 mM NaF, and 0.1 mM Na_3VO_4). Similarly, the whole-cell lysates
223 of uninfected TE671 and TE671/SFVmfu(PI) cells were obtained with RIPA buffer. The
224 lysates were mixed with Laemmli sample buffer supplemented with 2-mercaptoethanol and
225 boiled at 95°C for 5 min. Each boiled sample was electrophoresed on a sodium dodecyl
226 sulfate-polyacrylamide gel and electrically blotted onto a polyvinylidene difluoride
227 membrane. Each blotted membrane was blocked in 5% milk/Tris-buffered saline with
228 Tween 20 and incubated with an anti-CAP1 antibody (Abcam, Tokyo, Japan [catalog
229 number: EPR8339(B)]) as the primary antibody or a goat anti-rabbit IgG-horseradish
230 peroxidase antibody (Thermo Fisher Scientific [catalog number: 31466]) as the secondary
231 antibody. Antibody reactions were detected and processed with the SuperSignal West
232 Femto system (Thermo Fisher Scientific) using a Luminescent Image Analyzer LAS4000
233 mini (Fujifilm, Tokyo, Japan).
234
235 *RISC activity assay*
236 The RISC activity assay was conducted to verify that the miRNA expression plasmids
237 can produce the intended miRNAs. HEK293T cells in collagen-coated 24 well plates

238 (Iwaki, Shizuoka, Japan) were co-transfected with 40 ng of each firefly luciferase reporter
239 plasmid, 4 ng of pRL-TK (*Renilla* luciferase reporter plasmid) (Promega), and 456 ng of
240 each expression plasmid as indicated in Fig. 3B using Lipofectamine 2000 (Thermo Fisher
241 Scientific) according to the manufacturer's instruction. The cells were harvested 24 h after
242 transfection and were subjected to the luciferase assay with the Dual-Glo Luciferase
243 Assay System (Promega) using Lumat LB9507 (Berthold, Bad Wildbad, Germany). The
244 statistical significance was assessed using the Student's *t*-test.
245
246 *Host target 3′UTR luciferase assays*
247 HEK293T cells in collagen-coated 24 well plates (Iwaki) were co-transfected with 5 ng
248 of pGL3-hCMV/CAP1 3′UTR (either Wild-type, Single mut., or Triple mut.), 5 ng of pRL-TK
249 (Promega), and 790 ng of either empty plasmid (pUC18 or pcDNA3.1[+]) or each miRNA
250 expression plasmid as indicated in Fig. 4B in triplicate using the Lipofectamine 2000
251 (Thermo Fisher Scientific) according to the manufacturer's instruction. The cells were
252 harvested 24 h after transfection and were subjected to the luciferase assay with the Dual-
253 Glo Luciferase Assay System (Promega) using Lumat LB9507 (Berthold). The statistical
254 significance was assessed using the Student's *t*-test.
255 Uninfected TE671 and TE671/SFVmfu(PI) cells in collagen-coated 24 well plates
256 (Iwaki) were co-transfected with 80 ng of pGL3-hCMV/CAP1 3′UTR (either Wild-type,

257 Single mut., or Triple mut.), or pGL3-hCMV, 80 ng of pRL-TK, and 640 ng of the empty
258 plasmid (pcDNA3.1[+]) in triplicate using the Lipofectamine 2000 (Thermo Fisher
259 Scientific) to the manufacturer's instruction. The cells were harvested 24 h after
260 transfection and assayed for luciferase activity with the Dual-Glo Luciferase Assay System
261 (Promega) using Lumat LB9507 (Berthold). The statistical significance was assessed
262 using the Student's *t*-test.
263
264 *Accession numbers*
265 Illumina Hiseq sequencing data and nucleotide sequences identified in this study were
266 deposited to the database of the DNA Data Bank of Japan with the following accession
267 numbers: DRA008912, DRA008923, and LC498639.

Results

TE671 cells persistently infected with SFVmfu express viral miRNAs

The small RNA sequencing analyses were performed using the total RNAs extracted from both TE671 and TE671/SFVmfu(PI) cells. Almost all short reads (99.99%) obtained from uninfected TE671 cells were not mapped to the viral genome of SFVmfu, whereas approximately one-third of short reads (32.02%) obtained from TE671/SFVmfu(PI) cells were mapped to the viral genome of SFVmfu (Fig. 1A). As reported previously in SFVcae (Kincaid *et al.*, 2014), seven pre-miRNAs (S1–S7) and 14 mature-miRNAs were identified in SFVmfu, all of which are derived from the U3 region of LTR (Figs. 1B and S1, and Table 1). Moreover, pre-miRNAs identified contained A/B-box sequences, which are the promoter elements essential for initiating the transcription driven by RNA polymerase III (Figs.1C and S1) (Kassavetis and Geiduschek, 2006). These promoter elements were also identified in pre-miRNAs of SFVcae (Kincaid *et al.,* 2014). Among the 14 mature miRNAs identified, SFVmfu-miR-S7-5p which showed the highest expression was derived from a dumbbell-shaped pre-miRNA, SFVmfu-mir-S6-7 (Fig. 1C and Table 1). The seed sequence of the SFVmfu-miR-S7-5p (“GGAAUG”) was different from that of the SFVcae-miR-S7-5p (“AGAAGG”) (Fig. 1D). Notably, the miR-1 miRNA precursor family of the host has the same seed sequence with the SFVmfu-miR-S7-5p (Fig. 1D). This data indicates

286 that the SFVmfu-miR-S7-5p might share the same target genes with human miR-1 (hsa-
287 miR-1).
288
289 *CAP1 is downregulated by SFVmfu infection in TE671 cells*
290 To know the function of the SFVmfu-miR-S7-5p, transcriptome analysis was
291 performed in both TE671 and TE671/SFVmfu(PI) cells (Fig. 2A). Among the genes which
292 were predicted to be recognized by the SFVmfu-miR-S7-5p (highlighted with black dots in
293 Fig. 2A), the expression level of CAP1 was relatively high in uninfected TE671 cells but
294 low in TE671/SFVmfu(PI) cells (app. 75% reduction of FPKM). The immunoblot analysis
295 also indicated that the expression of CAP1 is severely downregulated at the protein level
296 by both acute and persistent infections with SFVmfu (Fig. 2B). The 3′UTR of CAP1
297 contains three potential SFVmfu-miR-S7-5p recognition sites, which are conserved across
298 and several primate species, including Japanese macaque and human (Fig. 2C).
299
300 *SFVmfu-miR-S7-5p downregulates a reporter gene with its complementary sequence in*
301 *3′UTR*
302 To investigate whether the constructed expression plasmids for SFVmfu-mir-S7-5p
303 and hsa-mir-1 (pUC18/SFVmfu-mir-S6-7 and pcDNA3.1(+)/hsa-mir-1, respectively)
304 produce target-specific miRNAs, the RISC activity assay was performed. A small part of

305 the U3 region of LTR in SFVmfu was used to construct the pUC18/SFVmfu-mir-S6-7
306 (containing the sequence of SFVmfu-miR-S7-5p) to avoid overlapping with other viral
307 miRNAs (Fig. 3A [center]). Reporter plasmids were also constructed, which contain the
308 complementary sequences of hsa-miR-1 and SFVmfu-miR-S7-5p downstream of the firefly
309 luciferase gene (Fig. 3A [bottom]). As a result, both miRNA expression plasmids
310 downregulated the expression of the reporter plasmids with complementary sequences
311 (Fig. 3B), indicating that both expression plasmids produce functional miRNAs (hsa-miR-1
312 and SFVmfu-miR-S7-5p, respectively) which silenced the mRNAs containing the
313 complementary sequences in the 3′UTR.
314
315 *SFVmfu-miR-S7-5p suppresses the CAP1 expression via recognition sites in 3′UTR*
316 To investigate whether SFVmfu-miR-S7-5p can recognize and downregulate the
317 expression of a gene bearing the 3′UTR of CAP1, we constructed a series of reporter
318 plasmids containing either wild-type or modified 3′UTR of CAP1 downstream of the firefly
319 luciferase gene (Fig. 4A). Both hsa-miR-1 and SFVmfu-miR-S7-5p repressed the
320 expression of the luciferase when the reporter plasmids contained the wild-type 3′UTR of
321 CAP1 (Fig. 4B). The level of luciferase expression was restored when the predicted
322 recognition sites were modified (Fig. 4B), suggesting that both hsa-miR-1 and SFVmfu-
323 miR-S7-5p repress the CAP1 expression via the recognition sites.

An additional reporter assay was carried out in TE671/SFVmfu(PI) cells without using the miRNA expression plasmids. TE671/SFVmfu(PI) cells, the level of luciferase expression was suppressed when the reporter plasmid contained the wild-type 3′UTR of CAP1, and the level of luciferase expression was restored when the recognition sites were disrupted (Fig. 4C). From these data, we concluded that TE671/SFVmfu(PI) cells express SFVmfu-miR-S7-5p which is capable of downregulating the CAP1 expression via the recognition sites.

Discussion

In this study, we showed that the persistent infection with SFVmfu in TE671 cells leads to the high expression of viral miRNAs encoded in the U3 region of SFVmfu LTR, as previously reported in SFVcae (Kincaid *et al.,* 2014) (Fig. 1). Among the miRNAs identified, we focused analyses on SFVmfu-miR-S7-5p, which had the highest read count among the 14 viral miRNAs identified (Fig. 1B). The multiple sequence alignment analysis of SFVs from *Macaca* species indicated that the U3 region of SFVmfu is distinct but comparable to those of SFVs from other macaques (rhesus and Taiwanese macaques [SFVmmu strain DPZ9524 and SFVmcy strain FV34, respectively]) (Fig. S2). Notably, the seed sequence ("GGAAUG") of miR-S7-5p of SFVmfu was the same with those of SFVmmu and SFVmcy, suggesting that they are also able to express the miRNA which harbors the same seed sequence with SFVmfu-miR-S7-5p. On the other hand, the seed sequence ("AGAAGG") of SFVcae-miR-S7-5p was remarkably different from that of SFVmfu-miR-S7-5p and expressed only moderately (Kincaid *et al.,* 2014). Instead, the cells infected with SFVcae express SFVcae-miR-S6-3p at a high level, which has the same seed sequence ("AACAGUC") with hsa-miR-132 (Kincaid *et al.,* 2014). Moreover, it was shown that both SFVcae-miR-S6-3p and hsa-miR-132 suppress the expression of EP300 (Kincaid *et al*., 2014), which is the transcriptional coactivator of the type-1 interferon response (Lagos *et al.,* 2010). However, the cells infected with SFVmfu express

350 SFVmfu-miR-S6-3p with a different seed sequence (“CGCUGCG”) only at a moderate
351 level (Figs. 1B and S2). Our transcriptome analyses indicated that the expression of
352 EP300 was not significantly changed by SFVmfu infection (data not shown). These data
353 suggest that the target genes regulated by miRNAs are different between SFVmfu and
354 SFVcae.
355 The expression of CAP1 was severely downregulated by SFVmfu-infection in TE671
356 cells (Fig. 2). In the luciferase reporter assay using the miRNA expression plasmids, the
357 luciferase activity of reporter plasmid containing CAP1 3′UTR was not fully recovered by
358 the disruption of all three predicted miRNA recognition sites (Fig. 4B). On the other hand,
359 when the reporter plasmids were transfected into TE671/SFVmfu(PI) cells, the luciferase
360 activity was fully recovered by the disruption of the three recognition sites (Fig. 4C). One
361 possible explanation for the discrepancy is that the use of the plasmid (pUC18) without
362 mammalian promoters might cause the non-specific suppression of firefly luciferase
363 protein produced from the pGL3-based reporter plasmids. Such an incomplete recovery by
364 the use of the plasmid without mammalian promoters in the luciferase reporter assay was
365 also observed in the previous report (Kincaid *et al.,* 2014). Nonetheless, the complete
366 recovery of relative luciferase activity, in the reporter assay using TE671/SFVmfu(PI) cells,
367 by the disruption of the three recognition sites indicates that the SFVmfu-miR-S7-5p
368 indeed downregulates the CAP1 through the predicted recognition sites in the cells.

Physiologically, CAP1 is involved in actin cytoskeleton remodeling in mammalian cells, and knock-down of CAP1 results in impaired cell migration with decreased actin depolymerization (Bertling *et al.,* 2004). Actin depolymerization plays a crucial role in the replication of retroviruses such as human immunodeficiency virus 1 (Yoder *et al*., 2008; Gladnikoff *et al*., 2009; Santos *et al*., 2012; Wen *et al.*, 2014). However, it is not clear at present whether the downregulation of CAP1 by the SFVmfu-miR-S7-5p benefits the replication strategy of the SFVmfu.

One possible hypothesis for the significance of SFV miRNAs is that the viral miRNAs contribute to the autoinhibitory regulation of the SFV gene expression in the infected cells. Intriguingly, the deletion of a 5′-portion of the U3 region (a possible miRNA cluster) in a chimpanzee-derived SFV leads to the increased viral replication in fibroblasts (Schmidt *et al.,* 1997). SFV might utilize the miRNAs to optimize the long-term co-existence with the host, as reported in other viruses such as herpes simplex virus 1 and polyomavirus (Umbach *et al.,* 2008; Broekema *et al.,* 2013).

Another hypothesis for the significance of SFV miRNAs is that the miRNAs of SFVs suppress the expression of genes that are involved in the development of cancers. Among family *Retroviridae*, gammaretroviruses preferentially integrate into the vicinity of TSSs of the host genes (Desfarges and Ciuffi, 2010). Such integration potentially leads to tumorigenesis when the integration occurred in the promoter/enhancer regions of proto-

388 oncogenes. Similar to gammaretroviruses, FVs also tend to integrate into the vicinity of
389 TSSs (Trobridge *et al.,* 2006). However, there is no report indicating the development of
390 cancers by SFV infection. Thus, SFVs might utilize unrevealed mechanisms to avoid the
391 development of cancers in the host primates. The SFVmfu-miR-S7-5p might counter the
392 development of tumors by repressing the expression of CAP1 in the infected cells. It is
393 interesting to note that the expression level of hsa-miR-1, which shares the seed
394 sequence with the SFVmfu-miR-S7-5p, is downregulated in various types of cancers (Liu
395 *et al.,* 2015; Han *et al.,* 2017; Korde *et al.,* 2017). Upregulation of CAP1 is observed in
396 several solid tumors, such as ovarian cancer, breast cancer (Xie *et al.,* 2014, 2018; Hua *et*
397 *al.,* 2015; Hasan and Zhou, 2019), and rhabdomyosarcoma from which the TE671 cell line
398 is derived (Rao *et al.,* 2010). Rhabdomyosarcoma is also known to have a reduced
399 expression level of hsa-miR-1, which suppresses the CAP1 expression (Vinther *et al.*,
400 2007; Rao *et al.,* 2010). Interestingly, the SFVcae-miR-S6-3p shares the seed sequence
401 with hsa-miR-132, which is also downregulated in several types of tumors (Formosa *et al.,*
402 2012; Wang *et al.,* 2014; Zhang *et al.,* 2016). SFVs might utilize distinct miRNAs to avoid
403 tumorigenesis by suppressing various onco-related genes.

Acknowledgments

We would like to thank the Japan Society for the Promotion of Science (JSPS) for providing financial supports for this project (KAKENHI Grant Numbers 16J10964, 17H03924, and 17H01048). A. H. -G. received financial support from JSPS Research Fellowship for Young Scientists.

409 **References**

410 Abdelfattah, A.M., Park, C., and Choi, M.Y. (2014) Update on non-canonical microRNAs.
411 Biomol Concepts 5: 275-287.

412 Bartel, D.P. (2009) MicroRNAs: target recognition and regulatory functions. *Cell* 136: 215-
413 233.

414 Bertling, E., Hotulainen, P., Mattila, P.K., Matilainen, T., Salminen, M., and Lappalainen, P.
415 (2004) Cyclase-associated protein 1 (CAP1) promotes cofilin-induced actin dynamics
416 in mammalian nonmuscle cells. Mol Biol Cell 15: 2324-2334.

417 Bolger, A.M., Lohse, M., and Usadel, B. (2014) Trimmomatic; a flexible trimmer for illumine
418 sequence data. Bioinformatics 30: 2114-2120.

419 Broekema, N.M., and Imperiale, M.J. (2013) miRNA regulation of BK polyoma-virus
420 replication during early infection. Proc Natl Acad Sci USA 110: 8200-8205.

421 Cao, W., Heit, A., Hotz-Wagenblatt, A., and Löchelt, M. (2018) Functional characterization
422 of the bovine foamy virus's miRNA expression cassette and its dumbbell-shaped pri-
423 miRNA. Virus Genes 54: 550-560.

424 Chen, S., Zhou, Y., Chen, Y., and Gu, J. (2018) Fastp: an ultra-fast all-in-one FASTQ
425 preprocessor. Bioinformatics 34: 884-890.

426 Chendrimada, T.P., Gregory, R.I., Kumaraswamy, E., Norman, J., Cooch, N., Nishikura,
427 K., and Shiekhattar, R. (2005) TRBP recruits the Dicer complex to Ago2 for microRNA
428 processing and gene silencing. Nature 436: 740-744.
429 Desfarges, S., and Ciuffi, A. (2010) Retroviral integration site selection. Viruses 2: 111-
430 130.
431 Eulalio, A., Huntzinger, E., Nishihara, T., Rehwinkel, J., Fauser, M., and Izaurralde, E.
432 (2009) Deadenylation is a widespread effect of miRNA regulation. RNA 15: 21-32.
433 Formosa, A., Lena, A.M., Markert, E.K., Cortelli, S., Miano, R., Mauriello, A., *et al.* (2012)
434 DNA methylation silences miR-132 in prostate cancer. Oncogene 32: 127-134.
435 Galvin, T.A., Ahmed, I.A., Shahabuddin, M., Bryan, T., and Khan, A.S. (2013) Identification
436 of recombination in the envelope gene of simian foamy virus serotype 2 isolated from
437 *Macaca cyclopis*. J Virol 87: 8792-8997.
438 Gladnikoff, M, Shimoni, E., Gov, N.S., and Rousso, I. (2009) Retroviral assembly and
439 budding occur through an actin-driven mechanism. Biophys J 97: 2419-2428.
440 Gouy. M., Guindon, S., and Gascuel, O. (2010) SeaView version 4: a multiplatform
441 graphical user interface for sequence alignment and phylogenetical tree building. Mol
442 Biol Evol 27: 221-224.
443 Graham, F.L., Smiley, J., Russell, W.C., and Nairn, R. (1977) Characteristics of a human
444 cell line transformed by DNA from human adenovirus type 5. J Gen Virol 1: 59-74.

445 Gruber, A.R., Lorenz, R., Bernhart, S.H., Neuböck, R., and Hofacker, I.L. (2008) The
446 Vienna RNA websuite. Nucleic Acids Res 36: W70-4.
447 Han, C., Shen, J.K., Hornicek, F.J., Kan, Q., and Duan, Z. (2017) Regulation of microRNA-
448 1 (miR-1) expression in human cancer. Biochim Biophys Acta 1860: 227-232.
449 Hasan, R., and Zhou, G.-L. (2019) The cytoskeletal protein cyclase-associated protein 1
450 (CAP1) in breast cancer: context-dependent roles in both the invasiveness and
451 proliferation of cancer cells and underlying cell signals. Int J Mol Med 20: E2653.
452 Hashimoto-Gotoh, A., Yoshikawa, R., and Miyazawa, T. (2015) Comparison between S+L-
453 assay and LacZ marker rescue assay for detecting replication-competent
454 gammaretroviruses. Biologicals 43: 363-368.
455 Hua, M., Yan, S., Yan, D., Xi, Q., Liu, R., Yang, S., *et al.* (2015) CAP1 is overexpressed in
456 human epithelial ovarian cancer and promotes cell proliferation. Int J Mol Med 35:
457 941-949.
458 Kassavetis, G.A., and Geiduschek, E.P. (2006) Transcription factor TFIIIB and
459 transcription by RNA polymerase III. Biochem Soc Trans 34: 1082-1087.
460 Katoh, K., and Standley, D.M. (2013) MAFFT multiple sequence alignment software
461 version 7: improvements in performance and usability. Mol Biol Evol 30: 772-780.
462 Khan, A.S., Bodem, J., Buseyne, J.F., Gessain, A., Johnson, W., Kuhn, J.H., *et al.* (2018)
463 Spumaretroviruses: updated taxonomy and nomenclature. Virology 516: 158-164.

464 Kim, D., Langmead, B., and Salzberg, S.L. (2015) HISAT: a fast spliced aligner with low
465 memory requirements. Nat Methods 12: 357-360.
466 Kincaid, R.P., Burke, J.M., and Sullivan, C.S. (2012) RNA virus microRNA that mimics a B-
467 cell oncomiR. Proc Natl Acad Sci USA 109: 3077-3082.
468 Kincaid, R.P., Chen, Y., Cox, J.E., Rethwilm, A., and Sullivana, C.S. (2014) Noncanonical
469 microRNA (miRNA) biogenesis gives rise to retroviral mimics of lymphoproliferative
470 and immunosuppressive host miRNAs. mBio 5: e00074.
471 Klase, Z., Kale, P., Winograd, R., Gupta, M.V., Heydarian, M., Berro, R., *et al.* (2007) HIV-
472 1 tar element is processed by dicer to yield a viral micro-RNA involved in chromatin
473 remodeling of the viral LTR. BMC Mol Biol 8: 63.
474 Korde, A., Jin, L., Zhang, J.G., Ramaswamy, A., Hu, B., Kolahian, S., *et al.* (2017) Lung
475 endothelial microRNA-1 regulates tumor growth and angiogenesis. Am J Respir Crit
476 Care Med 196: 1443-1455.
477 Lagos, D., Pollara, G., Henderson, S., Gratrix, F., Fabani, M., Milne, R.S.B., *et al.* (2010)
478 miR-132 regulates antiviral innate immunity through suppression of the p300
479 transcriptional co-activator. Nat Cell Biol 12: 513-519.
480 Lambert, C., Rua, R., Gessain, A., and Buseyne, F. (2016). A new sensitive indicator cell
481 line reveals cross-transactivation of the viral LTR by gorilla and chimpanzee simian
482 foamy viruses. Virology 496: 219-266.

483 Lander, M.R., and Chattopadhyay, S.K. (1984) A Mus dunni cell line that lacks sequences
484 closely related to endogenous murine leukemia viruses and can be infected by
485 ectropic, amphotropic, xenotropic, and mink cell focus-forming viruses. J Virol 52:
486 695-698.
487 Langmead, B., and Salzberg. S. (2012) Fast gapped-read alignment with bowtie2. Nat
488 Methods 9: 357-359.
489 Li, H., Handsaker, B., Wysoker, A., Fennel, T., Ruan, J., Homer, N., *et al.* (2009) The
490 sequence alignment/map format and SAMtools. Bioinformatics 25: 2078-2079.

491 Liu, T., Hu, K., Zhao, Z., Chen, G., Ou, X., Zhang, H., *et al.* (2015) MicroRNA-1 down-
492 regulates proliferation and migration of breast cancer stem cells by inhibiting the
493 Wnt/β-catenin pathway. Oncotarget 6: 41638-41649.

494 Liu, W., Worobey, M., Li, Y., Keele, B.F., Bibollet-Ruche, F., Guo, Y., *et al*. (2008)
495 Molecular ecology and natural history of simian foamy virus infection in wild-living
496 chimpanzees. PLoS Pathog 4: e1000097.
497 Liu, W., and Wang, X. (2019) Prediction of functional microRNA targets by integrative
498 modeling of microRNA binding and target expression data. Genome Biol 20: 18.
499 Lorenz, R., Bernhart, S. H., Shiederdissen, C.-H., Tafer, H., Flamm, C., and Stadler, P.F.
500 (2011) ViennaRNA Package 2.0. Algorithms Mol Biol 6: 26.

501 Miyazawa, T., Itagaki, S., Tomonaga, K., Ikeda, Y., Mori, T., Kawaguchi, Y., *et al.* (1995)
502 Establishment of carrier state infection of a feline renal cell line with feline syncytial
503 virus. J Vet Med Sci 57: 65-69.
504 Pinto-Santini, D.M., Stenbak, C.R., and Linial, M.L. (2017) Foamy virus zoonotic infections.
505 Retrovirology 14: 55.
506 Quinlan, A.R., and Hall, I.M. (2010) BEDtools: a flexible suite of utilities for comparing
507 genomic features. Bioinformatics 26: 841-842.
508 Rao, P.K., Missiaglia, E., Shields, L., Hyde, G., Yuan, B., Shepherd, C.J., *et al.* (2010)
509 Distinct roles for miR-1 and miR-133a in the proliferation and differentiation of
510 rhabdomyosarcoma cells. FASEB J 24: 3427-3437.
511 Sakaguchi, S., Okada, M., Shojima, T., Baba, K., and Miyazawa, T. (2008) Establishment
512 of LacZ marker rescue assay to detect infectious RD114 virus. J Vet Med Sci 70: 785-
513 790.
514 Santos, S., Obukhov, Y., Nekhai, S., Bukrinsky, M., and Iordanskiy, S. (2012) Virus-
515 producing cells determine the host protein profiles of HIV-1 virion cores. Retrovirology
516 9: 65.
517 Schmidt, M., Herchenroder, O., Heeney, J., and Rethwilm, A. (1997) Long terminal repeat
518 U3 length polymorphism of human foamy virus. Virology 230: 167-178.

519 Stratton, M.R., Darling, J., Pilkington, G.J., Lantos, P.L., Reeves, B.R., and Cooper, C.S.
520 (1989) Characterization of the human cell line TE671. Carcinogenesis 10: 889-905.
521 Switzer, W.M., Salemi, M., Shanmugam, V., Gao, F., Cong, M., Kuiken, C., *et al*. (2005)
522 Ancient co-speciation of simian foamy viruses and primates. Nature 434: 376-380.
523 Thompson, P.J., Macfarlan, T.S., and Lorincz, M.C. (2016) Long terminal repeats: from
524 parasitic elements to building blocks of the transcriptional regulatory repertoire. Mol
525 Cell 62: 766-776.
526 Trapnell, C., Williams, B., Pertea, G., Mortazavi, A., Kwan, G., Baren, J.V., *et al.,* (2010)
527 Transcript assembly and quantification by RNA-seq reveals unannotated transcripts
528 and isoforms switching during cell differentiation. Nat Biotechnol 28: 511-515.
529 Trapnell, C., Hendrickson, D., Sauvageau, M., Goff, L., Rinn, J.L., and Pachter, L. (2012)
530 Differential analysis of gene regulation at transcript resolution with RNA-seq. Nat
531 Biotechnol 31: 46-53.
532 Trobridge, G.D., Miller, D.G., Jacobs, M.A., Allen, J.M., Kiem, H.-P., Kaul, R., and Russell,
533 D.W. (2006) Foamy virus vector integration sites in normal human cells. Proc Natl
534 Acad Sci USA 103: 1498-1503.
535 Umbach, J.L., Kramer, M.F., Jurak, I., Karnowski, H.W., Coen, D.M, and Cullen, B.R.
536 (2008) MicroRNAs expressed by herpes simplex virus 1 during latent infection
537 regulate viral mRNAs. Nature 454: 780-783.

538 Vinther, J., Hedegaard, M.M., Gardner, P.P., Andersen, J.S., and Arctander, P. (2006)
539 Identification of miRNA targets with stable isotope labeling by amino acids in cell
540 culture. Nucleic Acid Res 34: e107.
541 Wang, J., Zu, G., Shen, F., and Kang, Y. (2014) miR-132 targeting cyclin E1 suppresses
542 cell proliferation in osteosarcoma cells. Tumor Biol 35: 4859-4865.
543 Wen, X., Ding, L., Wang, J.-J., Qi, M., Hammonds, J., Chu, H., *et al.* (2014) ROCK1 and
544 LIM kinase modulate retrovirus particle release and cell-cell transmission events. J
545 Virol 88: 6906-6921.
546 Whisnant, A.W., Kehl, T., Bao, Q., Maternial, M., Kuzmak, J., Löchelt, M., and Cullen, B.R.
547 (2014) Identification of novel, highly expressed retroviral microRNAs in cells infected
548 by bovine foamy virus. J Virol 88: 4679-4686.
549 Wong, N., and Wang, X. (2015) miRDB: an online resource for microRNA target prediction
550 and functional annotations. Nucleic Acid Res 43: 146-152.
551 Xie, S., Shen, C., Zhou, S., Xiong, M., Tan, M., Song, X., and Wang, C. (2018) Role of
552 adenylate cyclase-associated protein 1 in cancers. Int J Clin Exp Med 11: 3086-3099.
553 Xie, S.S., Tan, M., Lin, H.Y., Xu, L., Shen, C.X., Yuan, Q., *et al.* (2014) Overexpression of
554 adenylate cyclase-associated protein 1 may predict brain metastasis in non-small cell
555 lung cancer. Oncol Rep 33: 363-371.

556 Yao, Y., Smith, J.P., Nair, V., and Watson, M. (2014) An avian retrovirus uses canonical
557 expression and processing mechanisms to generate viral microRNA. J Virol 88: 2-9.
558 Yoder, A., Yu, D., Dong, L., Lyer, S.R., Xu, X., Kelly, J., *et al.* (2008) HIV envelope-CXCR4
559 signaling activates cofilin to overcome cortical actin restriction in resting CD4 T cells.
560 Cell 134: 782-792.
561 Yoshikawa, R., Nakagawa, S., Okamoto, M., and Miyazawa, T. (2014) Construction of an
562 infectious molecular clone of simian foamy virus of Japanese macaque (SFVjm) and
563 phylogenetic analysis of SFVjm isolates. Gene 548: 149-154.
564 Zhang, X., Tang, W., Li, R., He, R., Gan, T., Luo, Y., *et al.* (2016) Downregulation of
565 microRNA-132 indicates progression in hepatocellular carcinoma. Exp Ther Med 12:
566 2095-2101.
567

Table 1. List of mature miRNA sequences identified in this study

Name	Sequence (5'-3')	Length (nt)	Shape of pre-miRNA	Start position	End position	Number of reads
SFVmfu-miR-S1-5p	AGGAAGCAUUUGGUAAAUUCUAC	23	Dumbbell-shape with S2	10,476	10,498	121
SFVmfu-miR-S1-3p	UCAUUUACUACCGUGCUUCCGA	22		10,512	10,533	135,125
SFVmfu-miR-S2-5p	UGGAGAACUUAGGGACGAGGCU	22	Dumbbell-shape with S1	10,534	10,555	655,144
SFVmfu-miR-S2-3p	UCCUCAUCUCGAGUGUCUCCCUUU	24		10,571	10,594	20,786
SFVmfu-miR-S3-5p	AAGGGAGGGAGUGGAACGUCCUG	23	Single hairpin	10,658	10,680	35,207
SFVmfu-miR-S3-3p	UGACGCUCUCCCAUCCCUCCUUUUC	25		10,695	10,719	67,292
SFVmfu-miR-S4-5p	UCAAGAACCCAGGGAGCAAUGUUG	24	Single hairpin	10,842	10,865	250,036
SFVmfu-miR-S4-3p	AUAGUGCAUCCUGGUCGUUCUUUA	24		10,881	10,904	55,352
SFVmfu-miR-S5-5p	ACAAAGGGAAAUAGCUAAUGUGCA	24	Single hairpin	10,961	10,984	44
SFVmfu-miR-S5-3p	UACUUAGCCGUUCUCCUUUGAUA	23		10,999	11,021	91,370
SFVmfu-miR-S6-5p	AGGUGAAUGGCUCACAGUGAACGA	24	Dumbbell-shape with S7	11,120	11,143	57,461
SFVmfu-miR-S6-3p	UACGCUGCGUUGCCACCACCU	21		11,159	11,179	620,914
SFVmfu-miR-S7-5p	AGGAAUGCAGUGGGUAUGGAGUA	23	Dumbbell-shape with S6	11,182	11,204	1,014,472
SFVmfu-miR-S7-3p	UUCAUACUAACUACAUUCUUUU	22		11,222	11,243	434

568

Figure legends

Fig. 1. Persistent infection of SFVmfu leads to the expression of miRNAs at a high level. **(A)** Mapping of small RNAs in TE671 and TE671/SFVmfu(PI) cells to the genomes of SFVmfu and human. **(B)** Small RNA profiling of TE671/SFVmfu(PI) cells. The diagram above the graph shows the location of SFV genes and segments of LTR used for mapping. Fourteen types of mature miRNAs are indicated with arrows. **(C)** Predicted secondary structure of SFVmfu-mir-S6-7 identified in this study. Circles with solid, dashed, and dotted lines indicate the predicted A-box, B-box, and termination sequences, respectively. **(D)** Comparison of seed sequences of miR-S7-5p of SFVmfu and SFVcae with miR-1 miRNA precursor family (hsa-miR-1 and hsa-miR-206).

Fig. 2. Reduction of the expression of CAP1 by infection with SFVmfu in TE671 cells. **(A)** Total RNAs of uninfected TE671 and TE671/SFVmfu(PI) cells were extracted and subjected to transcriptome analyses. The gray and black dots indicate the genes that were predicted to have low and high affinities with SFVmfu-miR-S7-5p, respectively (see also Table S2.). **(B)** Immunoblot analyses to detect CAP1. TE671 cells that were either acutely (left panel) or persistently (right panel) infected with SFVmfu were subjected to the immunoblot analyses. The numbers on the lanes in the left panel indicate the h post-infection. Abbreviations: U.I.: uninfected TE671 cells; A.I.: TE671 cells acutely infected

588 with SFVmfu; P.I.: TE671/SFVmfu(PI) cells. **(C)** Three predicted recognition sites for
589 SFVmfu-miR-S7-5p present in CAP1 3′UTR from five different primate species. The
590 numbers above the alignment indicate the locations of CAP1 3′UTR in the human genome.
591
592 **Fig. 3.** RISC activity assays for the miRNA expression plasmids. **(A)** Expression plasmids
593 constructed for hsa-mir-1 (top) and SFVmfu-mir-S6-7 (center), and reporter plasmids
594 constructed for hsa-miR-1 and SFVmfu-miR-S7-5p (bottom). The backbone plasmid
595 (pUC18) for SFVmfu-mir-R6-7 does not contain mammalian promoters; however, the pre-
596 miRNA sequence contains the internal promoter elements (A/B-box sequences). The
597 reporter plasmids contain complementary sequences of mature miRNAs between the
598 firefly luciferase gene and poly(A) signal of the pGL3 vector inserted with the hCMV
599 enhancer/promoter. Sections cloned into the backbone plasmids are colored with grey. **(B)**
600 The RISC activity assays using the expression plasmids of hsa-miR-1 (left panel) and
601 SFVmfu-miR-S7-5p (right panel). Abbreviations: bGH: bovine growth hormone; SV: simian
602 virus 40.
603
604 **Fig. 4.** Suppression of the CAP1 expression by SFVmfu-miR-S7-5p via recognition sites.
605 **(A)** Reporter plasmids containing the 3′UTR of the CAP1 gene. Nucleotides shown in grey
606 characters indicate the mutated miRNA recognition sites. The numbers above the

alignment indicate the locations of CAP1 3′UTR in the human genome. **(B)** Luciferase reporter assay performed by co-transfection of miRNA expression plasmids with reporter plasmids. **(C)** Luciferase reporter assay performed in TE671/SFVmfu(PI) cells without using miRNA expression plasmids.

A

SFV-infection status	No. of total reads	Aligned 0 times	Aligned exactly 1 time	Aligned >1 times	Overall alignment to SFVmfu genome
Infected	10285829	6991429(67.97%)	3293348(32.02%)	1052(0.01%)	32.03%
Uninfected	10854004	10853382(99.99%)	622(0.01%)	0	0.01%

B

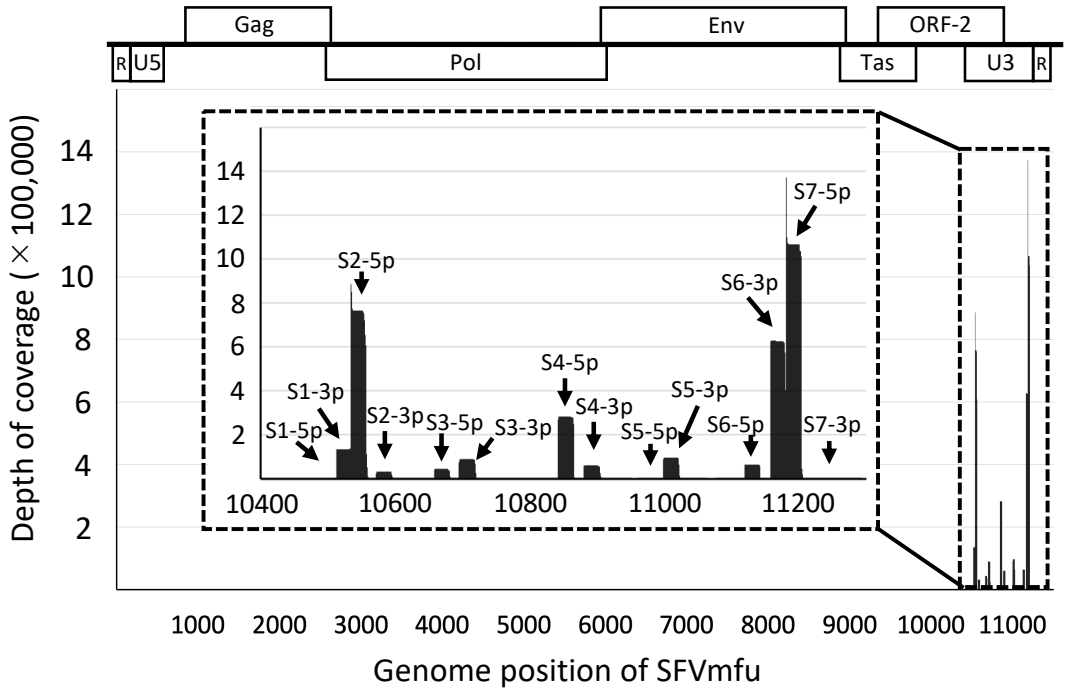

C

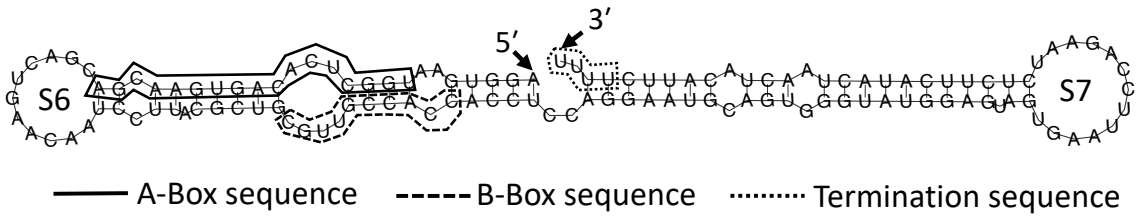

D

```
SFVcae-miR-S7-5p: 5′-AAGAAGGCCUCCAGAGUGAAAGA-3′
SFVmfu-miR-S7-5p: 5′-AGGAAUGCAGUGGGUAUGGAGUA-3′
      hsa-miR-1: 5′-UGGAAUGUAAAGAAGUAUGUAU-3′
    hsa-miR-206: 5′-UGGAAUGUAAGGAAGUGUGUGG-3′
                    Seed sequence
```

Fig. 1.

A

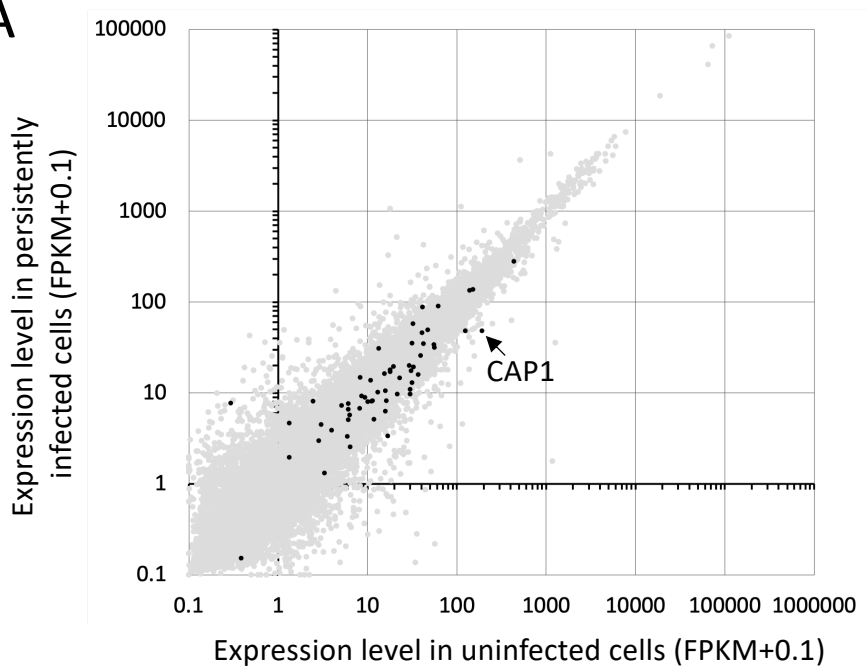
100000
10000
1000
100
10
1
0.1
0.1
1
10
100
1000
10000
100000
1000000
CAP1
Expression level in persistently infected cells (FPKM+0.1)
Expression level in uninfected cells (FPKM+0.1)

B

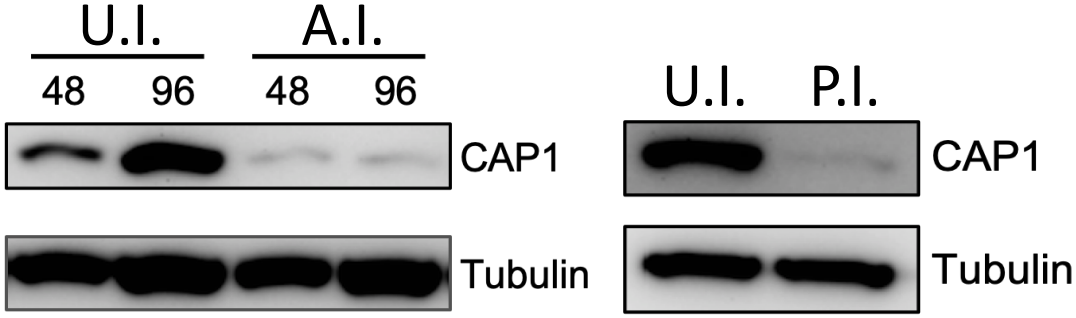
U.I.
A.I.
48
96
48
96
CAP1
Tubulin
U.I.
P.I.
CAP1
Tubulin

C

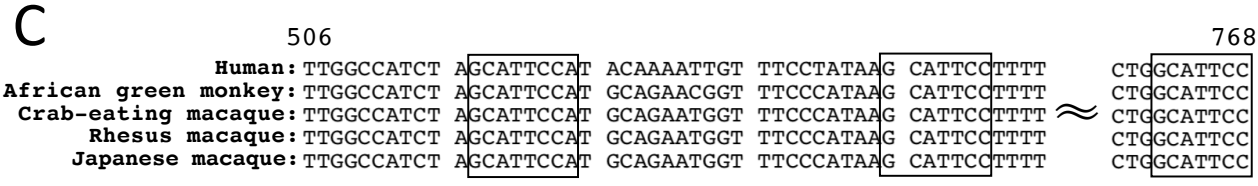
506
768
Human: TTGGCCATCT AGCATTCCAT ACAAAATTGT TTCCTATAAG CATTCCTTTT CTGGCATTCC
African green monkey: TTGGCCATCT AGCATTCCAT GCAGAACGGT TTCCCATAAG CATTCCTTTT CTGGCATTCC
Crab-eating macaque: TTGGCCATCT AGCATTCCAT GCAGAATGGT TTCCCATAAG CATTCCTTTT CTGGCATTCC
Rhesus macaque: TTGGCCATCT AGCATTCCAT GCAGAATGGT TTCCCATAAG CATTCCTTTT CTGGCATTCC
Japanese macaque: TTGGCCATCT AGCATTCCAT GCAGAATGGT TTCCCATAAG CATTCCTTTT CTGGCATTCC

Fig. 2.

A

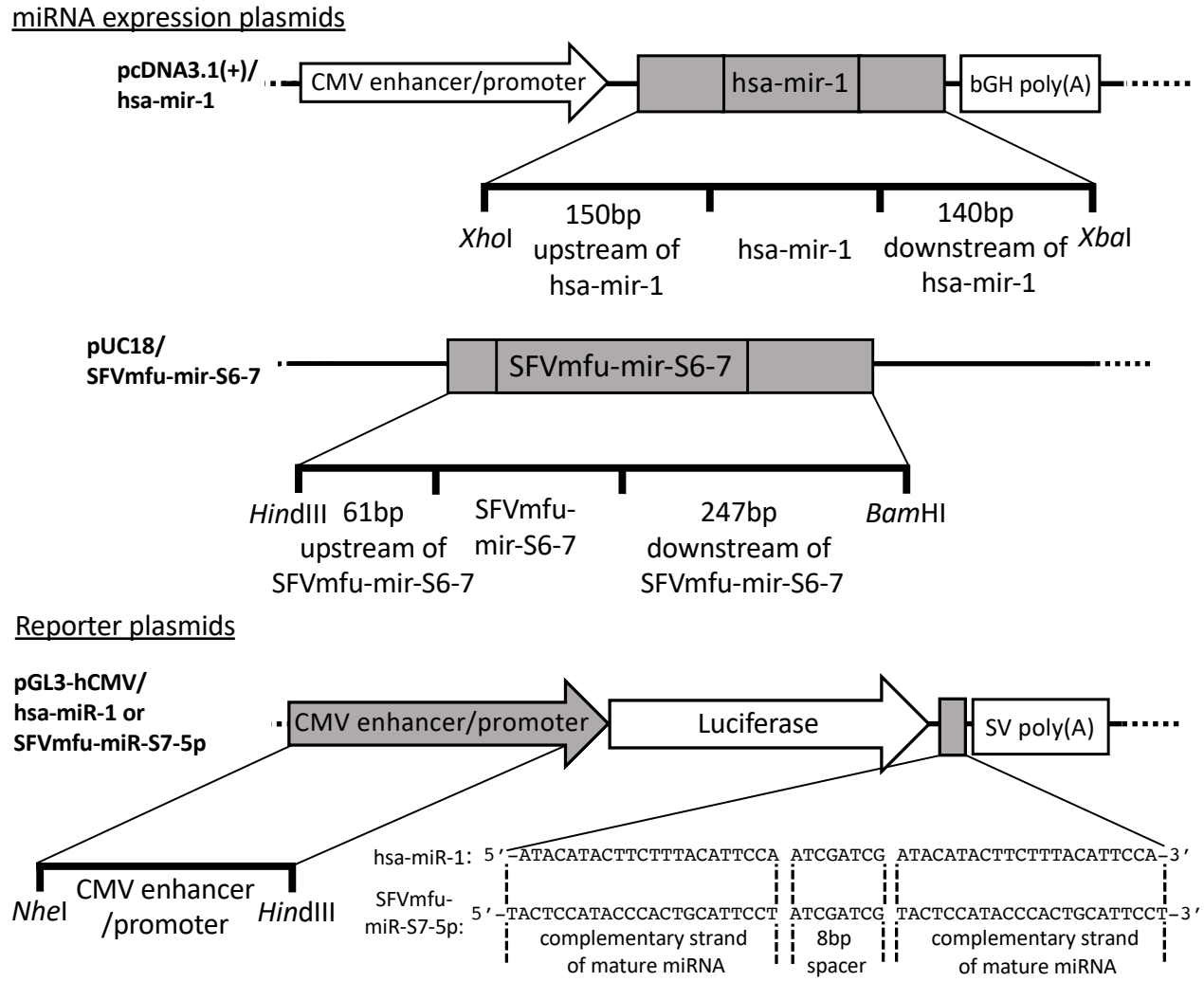
miRNA expression plasmids
pcDNA3.1(+)/
hsa-mir-1
CMV enhancer/promoter
hsa-mir-1
bGH poly(A)
XhoI
150bp
upstream of
hsa-mir-1
hsa-mir-1
140bp
downstream of
hsa-mir-1
XbaI
pUC18/
SFVmfu-mir-S6-7
SFVmfu-mir-S6-7
HindIII
61bp
upstream of
SFVmfu-mir-S6-7
SFVmfu-
mir-S6-7
247bp
downstream of
SFVmfu-mir-S6-7
BamHI
Reporter plasmids
pGL3-hCMV/
hsa-miR-1 or
SFVmfu-miR-S7-5p
CMV enhancer/promoter
Luciferase
SV poly(A)
NheI
CMV enhancer
/promoter
HindIII
hsa-miR-1: 5′–ATACATACTTCTTTACATTCCA ATCGATCG ATACATACTTCTTTACATTCCA–3′
SFVmfu-
miR-S7-5p: 5′–TACTCCATACCCACTGCATTCCT ATCGATCG TACTCCATACCCACTGCATTCCT–3′
complementary strand
of mature miRNA
8bp
spacer
complementary strand
of mature miRNA

B

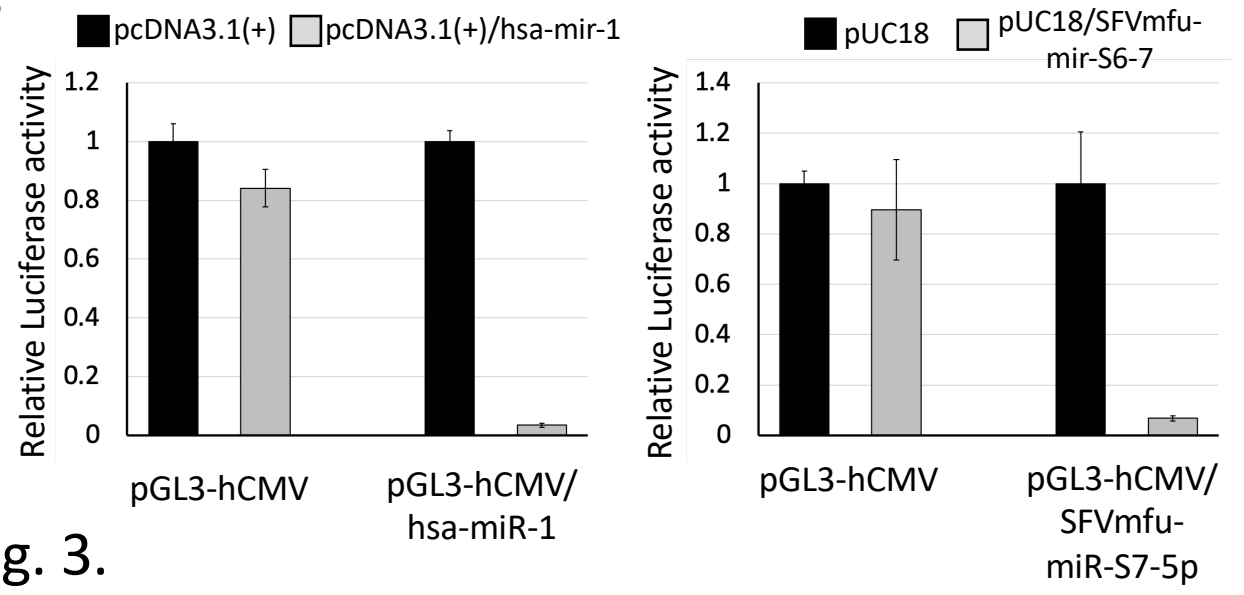
pcDNA3.1(+)
pcDNA3.1(+)/hsa-mir-1
Relative Luciferase activity
1.2
1
0.8
0.6
0.4
0.2
0
pGL3-hCMV
pGL3-hCMV/
hsa-miR-1
pUC18
pUC18/SFVmfu-
mir-S6-7
Relative Luciferase activity
1.4
1.2
1
0.8
0.6
0.4
0.2
0
pGL3-hCMV
pGL3-hCMV/
SFVmfu-
miR-S7-5p

Fig. 3.

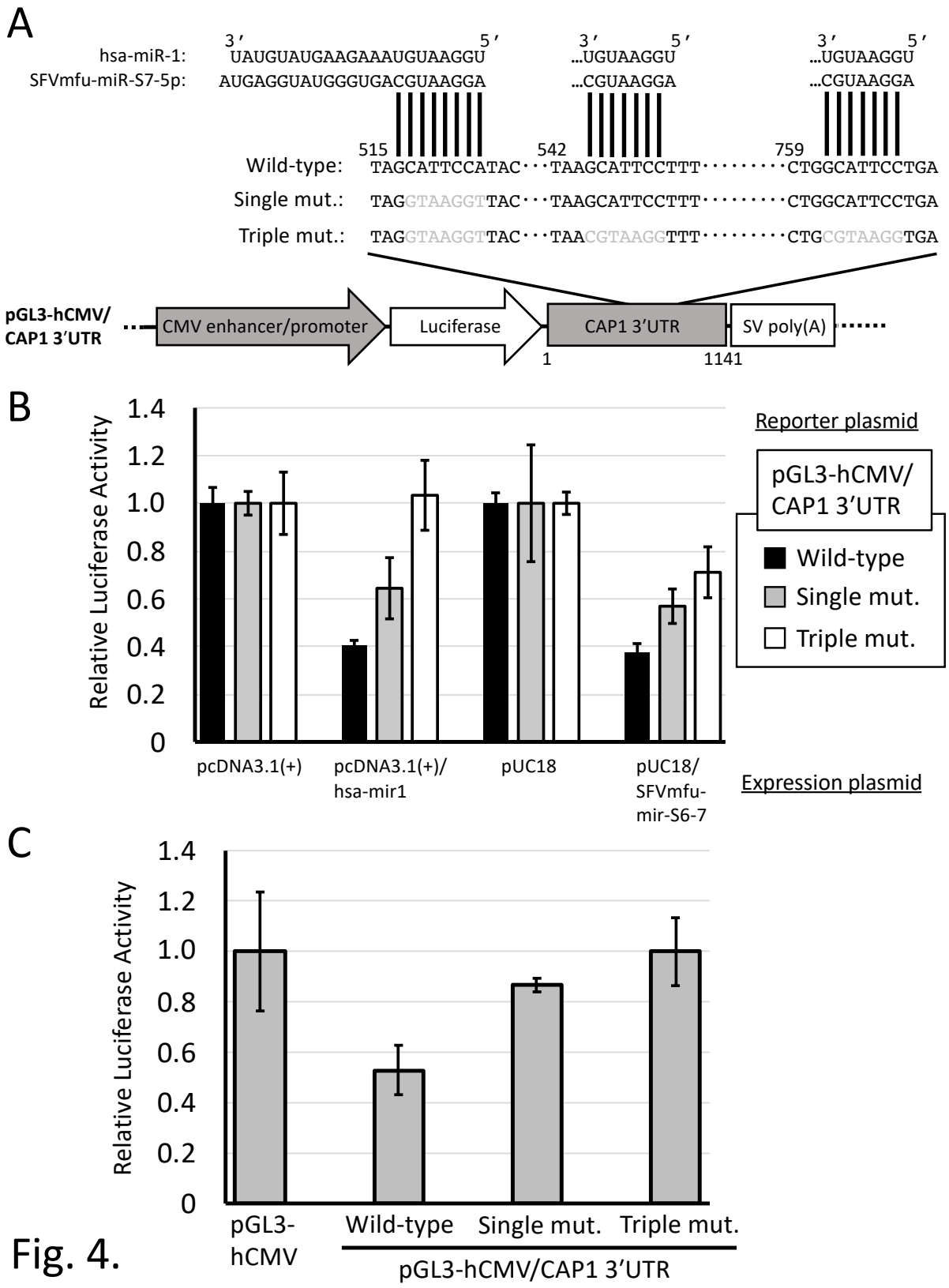
A
hsa-miR-1:
SFVmfu-miR-S7-5p:
3′
5′
UAUGUAUGAAGAAAUGUAAGGU
AUGAGGUAUGGGUGACGUAAGGA
…UGUAAGGU
…CGUAAGGA
515
542
759
Wild-type:
Single mut.:
Triple mut.:
TAGCATTCCATAC···TAAGCATTCCTTT·····CTGGCATTCCTGA
TAGGTAAGGTTAC···TAAGCATTCCTTT·····CTGGCATTCCTGA
TAGGTAAGGTTAC···TAACGTAAGGTTT·····CTGCGTAAGGTGA
pGL3-hCMV/
CAP1 3′UTR
CMV enhancer/promoter
Luciferase
CAP1 3′UTR
SV poly(A)
1
1141
B
Relative Luciferase Activity
1.4
1.2
1.0
0.8
0.6
0.4
0.2
0
Reporter plasmid
pGL3-hCMV/
CAP1 3′UTR
Wild-type
Single mut.
Triple mut.
pcDNA3.1(+)
pcDNA3.1(+)/
hsa-mir1
pUC18
pUC18/
SFVmfu-
mir-S6-7
Expression plasmid
C
Relative Luciferase Activity
1.4
1.2
1.0
0.8
0.6
0.4
0.2
0
pGL3-
hCMV
Wild-type
Single mut.
Triple mut.
pGL3-hCMV/CAP1 3′UTR

Fig. 4.

Supplementary materials

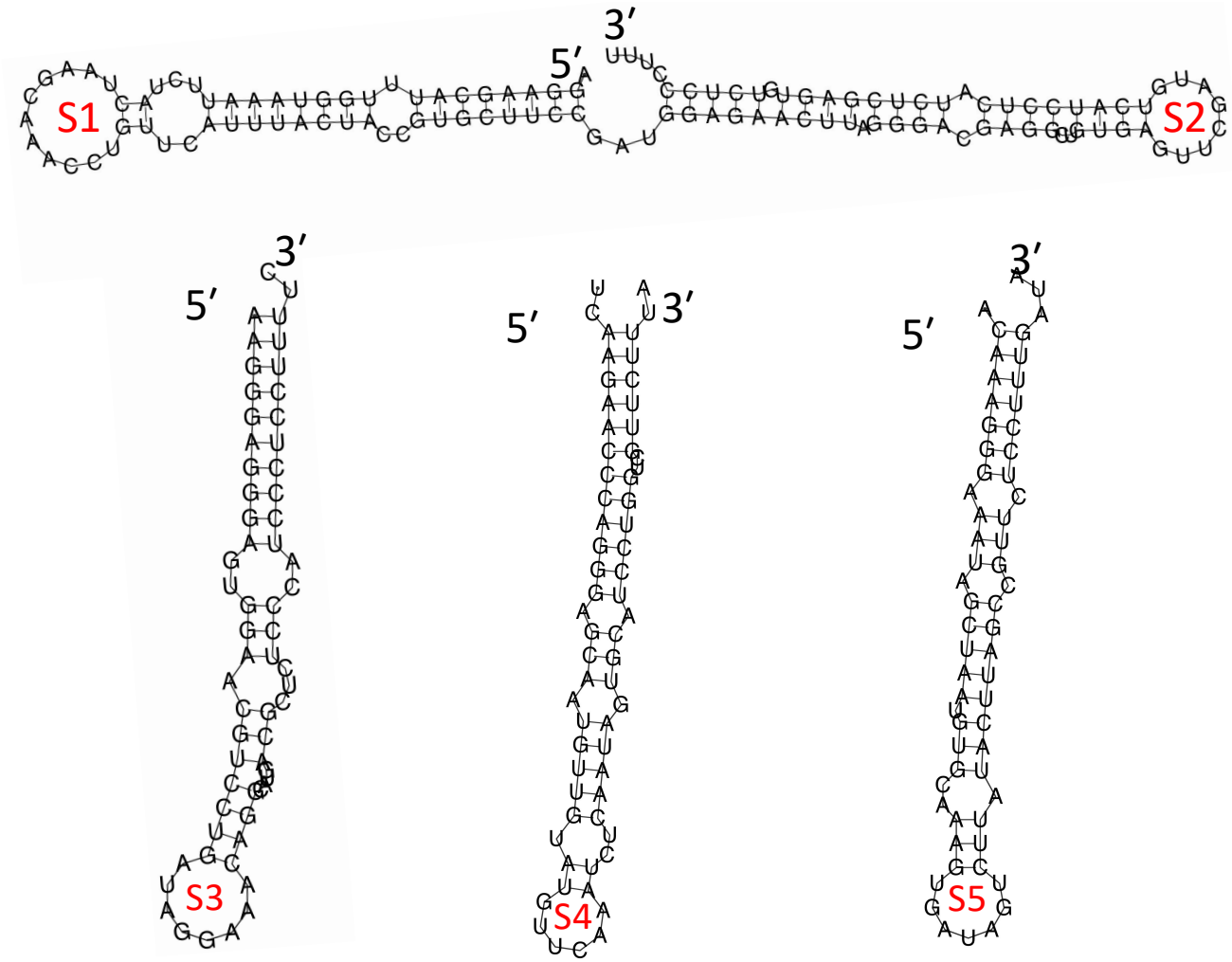

Fig. S1. The predicted secondary structures of pre-miRNA sequences of S1-2, S3, S4, and S5 identified in this study.

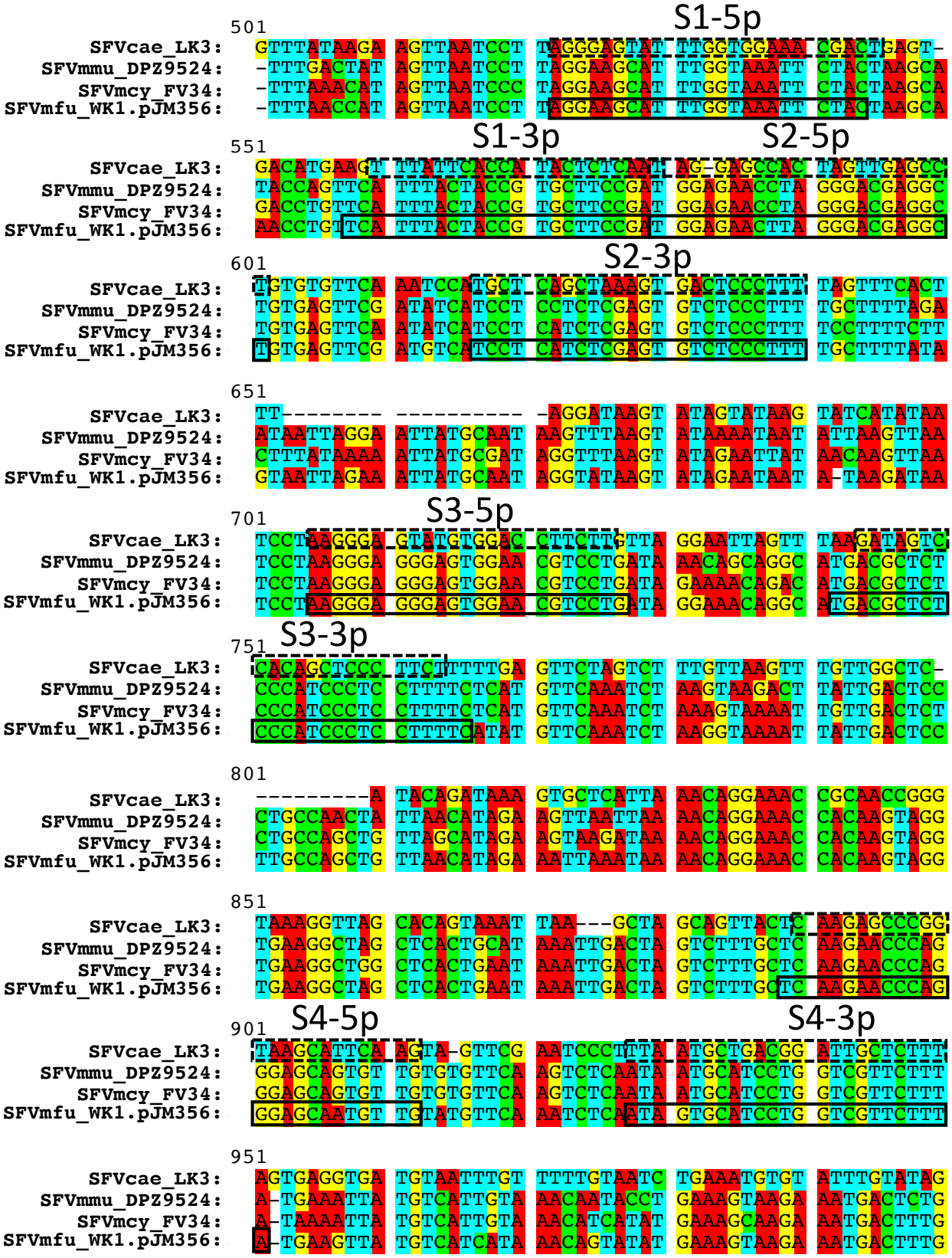

Fig. S2. The multiple sequence alignment of LTRs from SFVs from four primate species. The locations where the miRNAs were expressed are boxed with dotted and solid lines for SFVcae and SFVmfu, respectively.

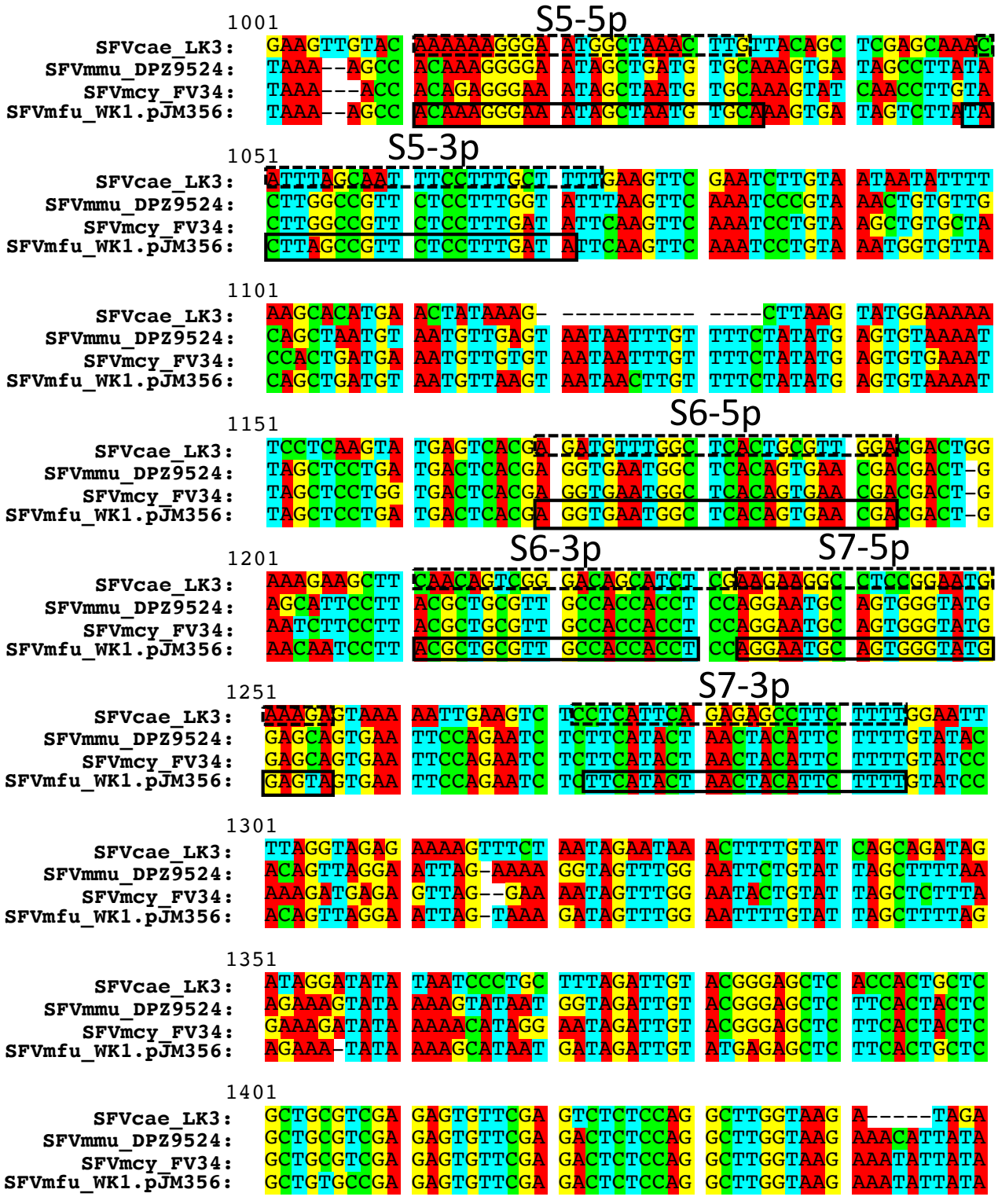

Fig. S2. (continued)

Table S1. Primers used in this study

Name	Purpose of PCR	Template	Target sequence	Sequence (5′ - 3′)
SFVmiRNA_S67_F	To construct miRNA expression plasmids	genomic DNA of TE671 cells infected with SFVmfu	pre-miRNA sequence of miRNA SFVmfu S6-7	CCCAAGCTTGTAATGTTAAGTAATAAGTTG
SFVmiRNA_S67_R				CGCGGATCCGCAGAGCATTAAAAGGATCAGAA
hsa-mir-1-F		genomic DNA of TE671 cells	pre-miRNA sequence of miRNA 1	ATCGCTCGAGGGCTGTCCTGCTCACACAGA
hsa-mir-1-R				CGATTCTAGAGCGGGGACACGACCGTCCAC
hCMVenh-Nhe1_F		pcDNA 3.1(+)	CMV enhancer and promoter	GCGAGCTAGCCAGATATACGCGTTGACATTG
hCMVpro-Hind3_R				TTAGAAGCTTAGCTCTGCTTATATAGACCTCCCA
miR1_comp_F	To construct luciferase reporter plasmids	No template (annealing and extending primers)	Complementary sequences of miRNA-1	GATCGCCGTGTAATTATACATACTTCTTTACATTCCAATCGATCGATACATACTTC
miR1_comp_R				CCGGCCGCCCCGACTTGGAATGTAAAGAAGTATGTATCGATCGATTGGAATGTAAA
SFV_S7-5'_comp_F		No template (annealing and extending primers)	Complementary sequences of miRNA SFVmfu S7-5p	GATCGCCGTGTAATTTACTCCATACCCACTGCATTCCTATCGATCGTACTC
SFV_S7-5'_comp_R				CCGGCCGCCCCGACTAGGAATGCAGTGGGTATGGAGTACGATCGATAGGAATG
CAP1_pGL3_3UTR_F		genomic DNA of TE671 cells	3′UTR of human CAP1 gene	GATCGCCGTGTAATTGCGAAGTGCCACTGGGTTC
CAP1_pGL3_3UTR_R				CCGGCCGCCCCGACTGCAAGTTTGGTATTAACTTTATTC
CAP1mut_F		pGL3-hCMV/CAP1 3′UTR (Wild-type)	3′UTR of human CAP1 gene	CTAGCAGTAAGGTTACAAAATTGTTTCC
CAP1mut_R				TGTAACCTTACCTAGATGGCCAAGCCTCAG
CAP1mut_2nd_F		pGL3-hCMV/CAP1 3′UTR (Single mut.)	3′UTR of human CAP1 gene	CTATAACGTAAGGTTTTATTCTCTATTC
CAP1mut_2nd_R				AAAACCTTACGTTATAGGAAACAATTTTG
CAP1mut_3rd_F		pGL3-hCMV/CAP1 3′UTR (Double mut.)	3′UTR of human CAP1 gene	AGTCTGCGTAAGGTGAATCCTTCTTCCC
CAP1mut_3rd_R				ATTCACCTTACGCAGACTCCTTGAAATC
Puro-InSIN_F	To obtain puromycin resistant gene	pMX-puro	puromycin resistant gene	CAGGATGAGGATCGTACCATGACCGAGTACAAGCCC
Puro-InSIN_R				GATAGAAGGCGATGCTCAGGCACCGGGCTTGCGG
CAP1-F	To sequence 3′UTR of CAP1 from Japanese macaque	Genomic DNA of Japanese macaque	3′UTR of CAP1 from Japanese macaque	CGCGAAGCTTGTTCAAGACCCTCTGGAATGGGCAG
CAP1-R				GGCAGAATTCGGATGTGAAAATAATTTTATGAGGT

Table S2. Predicted target genes of SFVmfu-miR-S7-5p obtained from miRDB (accessed in August 2019)

Target Rank	Gene Symbol	Target Score	Gene Description
1	MMD	100	monocyte to macrophage differentiation associated
2	CAP1	100	cyclase associated actin cytoskeleton regulatory protein 1
3	PTPRD	99	protein tyrosine phosphatase, receptor type D
4	SYT1	99	synaptotagmin 1
5	MCTP1	99	multiple C2 and transmembrane domain containing 1
6	CRIM1	98	cysteine rich transmembrane BMP regulator 1
7	GPR158	98	G protein-coupled receptor 158
8	SGK1	98	serum/glucocorticoid regulated kinase 1
9	XPO6	97	exportin 6
10	XPNPEP3	97	X-prolyl aminopeptidase 3
11	GLCCI1	97	glucocorticoid induced 1
12	ZFP36L2	97	ZFP36 ring finger protein like 2
13	USP46	97	ubiquitin specific peptidase 46
14	SMIM14	97	small integral membrane protein 14
15	SLC39A10	97	solute carrier family 39 member 10
16	EML4	97	EMAP like 4
17	AP3S1	97	adaptor related protein complex 3 subunit sigma 1
18	COL25A1	97	collagen type XXV alpha 1 chain
19	GJA1	97	gap junction protein alpha 1
20	GOLPH3	96	golgi phosphoprotein 3
21	NOTCH3	96	notch 3
22	PDCD4	96	programmed cell death 4
23	MTX1	96	metaxin 1
24	PABPC1	95	poly(A) binding protein cytoplasmic 1
25	KAT6A	95	lysine acetyltransferase 6A
26	WDR47	95	WD repeat domain 47
27	NCOA1	95	nuclear receptor coactivator 1
28	SS18	95	SS18, nBAF chromatin remodeling complex subunit
29	GNPTAB	95	N-acetylglucosamine-1-phosphate transferase subunits alpha and beta
30	BTAF1	95	B-TFIID TATA-box binding protein associated factor 1
31	ADAR	95	adenosine deaminase, RNA specific
32	ZNF281	94	zinc finger protein 281
33	GCLC	94	glutamate-cysteine ligase catalytic subunit
34	NPHS1	94	NPHS1, nephrin
35	TFE3	94	transcription factor binding to IGHM enhancer 3
36	TMIGD3	94	transmembrane and immunoglobulin domain containing 3
37	GLCE	94	glucuronic acid epimerase
38	ARHGAP32	94	Rho GTPase activating protein 32
39	POGK	93	pogo transposable element derived with KRAB domain
40	C4orf19	93	chromosome 4 open reading frame 19
41	PTPN14	93	protein tyrosine phosphatase, non-receptor type 14
42	HP1BP3	93	heterochromatin protein 1 binding protein 3
43	SLC44A2	93	solute carrier family 44 member 2
44	ARF4	93	ADP ribosylation factor 4
45	SLC44A1	93	solute carrier family 44 member 1
46	TSHR	93	thyroid stimulating hormone receptor
47	SLC10A7	93	solute carrier family 10 member 7
48	LRCH1	92	leucine rich repeats and calponin homology domain containing 1
49	PDIK1L	92	PDLIM1 interacting kinase 1 like
50	FAM102A	92	family with sequence similarity 102 member A
51	KDELR2	92	KDEL endoplasmic reticulum protein retention receptor 2
52	PDLIM2	92	PDZ and LIM domain 2
53	SEPHS2	92	selenophosphate synthetase 2
54	PPRC1	92	peroxisome proliferator-activated receptor gamma, coactivator-related 1
55	SERP1	92	stress associated endoplasmic reticulum protein 1
56	GNPDA2	91	glucosamine-6-phosphate deaminase 2
57	ATP6V1B2	91	ATPase H+ transporting V1 subunit B2
58	STAG2	91	stromal antigen 2
59	COG3	91	component of oligomeric golgi complex 3
60	NECTIN2	91	nectin cell adhesion molecule 2
61	KLF15	91	Kruppel like factor 15
62	HIGD1A	91	HIG1 hypoxia inducible domain family member 1A
63	HMBOX1	91	homeobox containing 1
64	PGBD5	91	piggyBac transposable element derived 5
65	ZNF326	91	zinc finger protein 326
66	HAND2	91	heart and neural crest derivatives expressed 2
67	ACVR1	90	activin A receptor type 1
68	AFF3	90	AF4/FMR2 family member 3
69	CLTC	90	clathrin heavy chain
70	UNK	90	unk zinc finger
71	TRPC7	90	transient receptor potential cation channel subfamily C member 7
72	C2CD4B	90	C2 calcium dependent domain containing 4B
73	CLCN5	90	chloride voltage-gated channel 5